

EVALUATION OF THE BOND AND TENSILE STRENGTH OF GFRP BARS EXPOSED
TO HARSH ENVIRONMENT

by

Saber Abedi

A Thesis Presented to the Faculty of the
American University of Sharjah
College of Engineering
in Partial Fulfillment
of the Requirements
for the Degree of

Master of Science in
Civil Engineering

Sharjah, United Arab Emirates

January 2014

Approval Signatures

We, the undersigned, approve the Master's Thesis of Saber Abedi.

Thesis Title: Evaluation of the Bond and Tensile Strength of GFRP Bars Exposed to Harsh

Environment

Signature

Date of Signature
(dd/mm/yyyy)

Dr. Adil K. Al-Tamimi
Professor, Department of Civil Engineering
Thesis Advisor

Dr. Farid H. Abed
Associate Professor, Department of Civil Engineering
Thesis Co-Advisor

Yehia
Associate Professor, Department of Civil Engineering
Thesis Co-Advisor

Dr. Mohammad AlHamaydeh
Associate Professor, Department of Civil Engineering
Thesis Committee Member

Dr. Shivakumar Ranganathan
Assistant Professor, Department of Mechanical Engineering
Thesis Committee Member

Dr. Aliosman Akan
Head, Department of Civil Engineering

Dr. Hany El-Kadi
Associate Dean, College of Engineering

Dr. Sherif

Dr. Leland Thomas Blank
Dean, College of Engineering

Dr. Khaled Assaleh
Director, Graduate Studies

Acknowledgements

I would like to express my gratitude to my thesis supervisors, committee members, family, and friends, without whom the completion of this research would have never been possible. Words are not enough to express my feelings to people who helped me to reach what I have always been dreaming about. First and foremost, I would like to thank my thesis supervisor, Dr. Adil Al-Tamimi for his supervision, motivation, and guidance throughout the research program, for believing in my ability to finish this project and guiding me through the right path to success. I am also grateful to my thesis co-advisors, Drs. Farid H. Abed and Sherif Yehia for their supportive comments and encouragements. I would also like to acknowledge Eng. Arshi Faridi and Eng. Mohammad Ansari for their support during the experimental stage of this research for supervising and controlling the experiment trials. I would like to thank Conmix, BASF, and Pultron companies, for providing us with concrete, epoxy, and GFRP bars to conduct the experiments. Many thanks also go to my parents for their love and support. They truly helped me to see myself achieving my goals. Finally, I would like to acknowledge my true friends, Sina Shabani, Shahin Dehbashi and Amin Bigdeli for their honest feedback and encouragement to finish this research during the entire Master's program.

Dedicated to my parents, without whom none of my success would be possible

Abstract

Fiber-reinforced polymers (FRP) have become one of the fastest-emerging materials to compete with conventional steel bars for use in concrete. The mechanical properties and durability of FRP materials are the main concerns that require attention. Different characteristics of FRP should be considered when estimating the service life of these polymers because they are relatively new materials in the Middle East region. By knowing the reduction in the mechanical properties of FRP bars, the durability of the bars can be predicted using data from short-term evaluation. In this thesis, the bond and tensile strength of the bars are examined before and after exposure to various conditions in order to reveal possible deterioration. The emphasis of this research is mainly on the evaluation of glass fiber-reinforced polymer (GFRP) bars exposed to harsh environmental conditions such as the splash zones that simulate seawater immersion, high temperatures combined with high moisture, and high alkalinity. Short-term behavior of GFRP bars can be established by comparing conditioned specimens vs. unconditioned specimens. The Arrhenius equation is used to find the long-term behavior of the GFRP materials. In this study, GFRP bars were kept in different environments for three different intervals: 30, 60, and 90 days. Uniaxial and pullout tests were conducted after each exposure to measure the tensile and bond strength. The alkaline solution was the most damaging environment for the bond strength of GFRP bars with a 33.6% reduction. Tensile strength was most affected by the seawater simulation environment, which caused a 13.31% reduction. Arrhenius modeling showed that a GFRP bar required 61 days to reach 90% of its initial bond strength, and 8.5 years to reach 70% of its initial tensile strength when the bar was exposed to high temperature.

Search Terms: GFRP, Bond, Tensile, Harsh environment, Arrhenius equation

Table of Contents

Abstract.....	7
---------------	---

List of Figures	9
List of Tables	13
Chapter 1: Introduction	15
1.1. Background	15
1.2. Research Objectives	17
Chapter 2: Literature Review	18
2.1. Bond Strength	18
2.2. Tensile Strength	24
Chapter 3: Material and Environment Preparations	28
3.1. Concrete Wooden Forms	28
3.2. GFRP Bars	28
3.3. Splash Zone Exposure	29
3.4. Alkaline Solution Exposure	29
3.5. High Temperature and Humidity Exposure	30
Chapter 4: Research Methodology	31
4.1. Characteristics of the Materials	31
4.1.1. Concrete	31
4.1.2. GFRP	33
4.1.3. Epoxy	34
4.2. Pullout Test	35
4.3. Tensile Test	38
Chapter 5: Results and Discussion	41
5.1. Pullout Test	41
5.2. Tensile Test	47
5.3. Arrhenius Modeling	52
Chapter 6: Conclusions and Recommendations	57
6.1. Conclusions	57

6.2. Recommendations.....	59
References.....	59
Appendix.....	62
A. Temperature and Humidity	62
B. Pullout Test Graphs.....	65
Vita.....	76

List of Figures

Figure 2.1: Bond-Strength Evolution of Conditioned GFRP Bars at 23 °C, 40 °C, and 50 °C [11] 19

Figure 2.2: Types of GFRP Bars Used in the Experiment [12] 20

Figure 3.1: Samples of Cubical Wooden Forms Prepared for the Pullout Test 26

Figure 3.2: GFRP Bars before Exposure 26

Figure 3.3: AUS Sustainability Center for Simulating the Splash Zone 27

Figure 3.4: GFRP Bars Exposed to the Alkaline Environment 27

Figure 3.5: Laboratory Grade Sodium Hydroxide Pellets 28

Figure 3.6: Variations in Temperature during the Exposure of Bars 28

Figure 3.7: Variations in Humidity during the Exposure of Bars 29

Figure 4.1: Concrete 1450i Container 33

Figure 4.2: Pullout Test Specification [24] 34

Figure 4.3: Samples of Cubic Wooden Forms Prepared before Casting Concrete 35

Figure 4.4: Samples after Casting 35

Figure 4.5: Pullout Test Setup 36

Figure 4.6: ASTM D638–10 Standards for Tensile Test [25] 37

Figure 4.7: GFRP Bars after Cutting 38

Figure 4.8: Steel Grips for Gripping Both Ends of GFRP Bars during the Uniaxial Test..... 38

Figure 4.9: GFRP Bar Tensile Test Setup 39

Figure 5.1: Complete Pullout

Failure.....	41	Figure 5.2: Failure of the
Concrete Cover	41	
Figure 5.3: Concrete Block Split	42	
Figure 5.4: Load-Extension Relationship of GFRP Bar Exposed to the Sun after 30 Days....	42	
Figure 5.5: Maximum Load for Each Specimen after the Pullout Test	43	
Figure 5.6: Bond Stress for Each Specimen	43	
Figure 5.7: Percentage Retention of Bond Stress for Different Type of Exposures	44	
Figure 5.8: Retention of Bond Stress of GFRP Bars Exposed to Sun	45	
Figure 5.9: GFRP Bar Mode of Failure after a Tensile Test	45	
Figure 5.10: Stress-Strain Relationship of Unconditioned GFRP	47	
Figure 5.11: Maximum Tensile Stress for Different Types of Exposures	48	
Figure 5.12: Percentage Retention of Tensile Stress for Different Types of Exposures in Current Study	48	
Figure 5.13: Retention of Tensile Strength of GFRP Bars Exposed to Sun Compared to Previous Study	49	
Figure 5.14: Retention of Tensile Strength of GFRP Bars Exposed to Seawater Solution Compared to Previous Study	49	
Figure 5.15: Retention of Tensile Strength of GFRP Bars Exposed to Alkaline Solution Compared to Previous Study	50	Figure
Figure 5.16: Regression Analysis for Bond Strength	52	
Figure 5.17: Regression Analysis for Tensile Strength	52	
Figure 5.18: Arrhenius Plots of Bond Strength Degradation	53	
Figure 5.19: Arrhenius Plots of Tensile Strength Degradation	53	
Figure 5.20: Long-term Performance of the		

Bond Strength of GFRP Bars	54	Figure 5.21: Long-term Performance of the Tensile Strength of GFRP Bars	54
Relationship of Unexposed GFRP Bar (Sample 1)	64	Figure B.1: Load-Extension Relationship of Unexposed GFRP Bar (Sample 1)	64
Figure B.2: Load-Extension Relationship of Unexposed GFRP Bar (Sample2)	64		
Figure B.3: Load-Extension Relationship of GFRP Bar Exposed to the Sun after 30 Days (Sample 1)	65		
Figure B.4: Load-Extension Relationship of GFRP Bar Exposed to the Sun after 30 Days (Sample 2)	65		
Figure B.5: Load-Extension Relationship of GFRP Bar Exposed to the Sun after 60 Days (Sample 1)	66		
Figure B.6: Load-Extension Relationship of GFRP Bar Exposed to the Sun after 60 Days (Sample 2)	66		
Figure B.7: Load-Extension Relationship of GFRP Bar Exposed to the Sun after 90 Days (Sample 1)	67		
Figure B.8: Load-Extension Relationship of GFRP Bar Exposed to the Sun after 90 Days (Sample 2)	67		
Figure B.9: Load-Extension Relationship of GFRP Bar Exposed to the Salt Solution after 30 Days (Sample 1)	68		
Figure B.10: Load-Extension Relationship of GFRP Bar Exposed to the Salt Solution after 30 Days (Sample 2)	68		
Figure B.11: Load-Extension Relationship of GFRP Bar Exposed to the Salt Solution after 60 Days (Sample 1)	69		
Figure B.12: Load-Extension Relationship of GFRP Bar Exposed to the Salt Solution after 60 Days (Sample 2)	69		
Figure B.13: Load-Extension Relationship of GFRP Bar Exposed to the Salt Solution after 90 Days (Sample 1)	70		

Figure B.14: Load-Extension Relationship of GFRP Bar Exposed to the Salt Solution after 90 Days (Sample 2)	70
Figure B.15: Load-Extension Relationship of GFRP Bar Exposed to the Alkaline Solution after 30 Days (Sample 1)	71
Figure B.16: Load-Extension Relationship of GFRP Bar Exposed to the Alkaline Solution after 30 Days (Sample 2)	71
Figure B.17: Load-Extension Relationship of GFRP Bar Exposed to the Alkaline Solution after 60 Days (Sample 1)	72
Figure B.18: Load-Extension Relationship of GFRP bar Exposed to the Alkaline Solution after 60 Days (Sample 2)	72
Figure B.19: Load-Extension Relationship of GFRP bar Exposed to the Alkaline Solution after 90 Days (Sample 1)	73
Figure B.20: Load-Extension Relationship of GFRP bar Exposed to the Alkaline Solution after 90 Days (Sample 2)	73

List of Tables

Table 1.1: Properties of steel and different FRP materials [8]	14
Table 2.1: FRP Rod Properties [9]	16
Table 2.2: Material Aspects of FRP Specimens [10]	17

Table 2.3: Compositions of Solution 2 to Solution 5 [10]	17
Table 2.4: Characteristics of the GFRP Bars Used in the Study, (Manufacturer’s Data) [12]	19
Table 2.5: Bond strength of GFRP Bars Exposed to Different Solutions in Various Studies .	22
Table 2.6: Tensile Strength of GFRP Bars Exposed to Different Solutions in Various Studies	25
Table 4.1: Concrete Mix Design Specifications (Conmix Company)	30
Table 4.2: Concrete Mix Design Detailed Specifications (Conmix Company)	31
Table 4.3: Mechanical and Physical Properties of GFRP Bar	32
Table 4.4: Setting Time of the Concreive 1450i	32
Table 4.5: Number of Specimens and Duration of the Exposure	33
Table 5.1: Maximum Load, Bond Strength, and Failure Type of the Specimens after Pullout Test	40
Table 5.2: Maximum Load and Tensile Strength Capacity for all GFRP Specimens	46
Table 5.3: Service Life Prediction of GFRP Bars for Different Type of Exposures	55
Table A.1: Variation of Temperature and Humidity during the Exposure of GFRP Bars	61

Chapter 1: Introduction

1.1. Background

Ensuring the durability and sustainability of materials is becoming the most challenging concern in the construction materials field. During the last two decades, researchers have found that fiber-reinforced polymers (FRP) can be used in place of traditional steel bars to reduce the problems associated with corrosion of steel [1]. Other advantages of FRPs are recognized, such as their ability to sustain a high tensile load (nearly double that of a steel bar), their flexibility, their ease of use and low environmental impact, and their light weight (one FRP bar weighs approximately one fourth as much as a steel bar with the same dimensions [2]). Carbon and glass are the most commonly used FRPs in today's structures. However, the low cost of glass FRPs (GFRPs) results in their wider use compared to carbon FRPs (CFRPs).

The most critical and unclear issue regarding the use of these materials is their durability under harsh environmental conditions [3]. GFRP reinforcements are mainly used in bridges and parking garages. Different environments and loading situations can affect the properties of the GFRP reinforcement and of the concrete itself, especially when the structure is located in an open area and is subjected to different kinds of exposures [4]. Chlorides and carbonation, which reduce the alkalinity of concrete, do not affect the durability of GFRP bars; however, field conditions have a significant effect on concrete durability [5]. Occasionally, the strength of reinforcing bars is reduced even before they are used in construction.

Different criteria may affect these bars, such as the storage environment or a high pH during the casting of concrete. The pH of fresh concrete is approximately 12.6 due to the presence of calcium hydroxide, $\text{Ca}(\text{OH})_2$, which forms during the hydration of cement. Dissolution of the calcium hydroxide creates hydroxyl ions in the pore water, which give concrete its high pH. Calcium hydroxide can undergo a reaction with carbon dioxide from the atmosphere to produce calcium carbonate (CaCO_3). This conversion of calcium hydroxide to calcium carbonate influences the surrounding fluid pH, which falls to about 8.3.

GFRP bars are anisotropic materials, with the longitudinal axis being the strongest. The diameter of the bar is important because an increase in the bar diameter will result in a decrease in tensile strength [6]. Different types of glass fibers are also available commercially for structural uses, such as E-glass, S-glass, C-glass, and AR-glass. E-glass is used in structures because of its high modulus and high electrical and acid resistance. S-glass, however, has higher stiffness compared to E-glass, but costs more, making it less competitive than E-glass. C-glass, on the other hand, is used for its chemical stability in harsh environments, while AR-glass is mainly used in alkaline environments that negatively affect the strength of the other types of glass fibers. Among all the available types of glass fibers, E-glass is the most effective and economical type for use in structures.

One of the most common uses of GFRP bars is in bridge decks, where they are an effective alternative to steel bars. They are lighter than steel, which makes their transportation easier and more economical. Moreover, the dead load on the bridge structure is reduced due to the lightweight nature of the glass fibers [7]. Table 1.1 shows a comparison of the properties of steel and other FRP materials.

Table 1.1: Properties of steel and different FRP materials [7]

	Steel	GFRP	CFRP	AFRP
Nominal yield stress, ksi (MPa)	40 to 75 (276 to 517)	N/A	N/A	N/A
Tensile strength, ksi (MPa)	70 to 100 (483 to 690)	70 to 230 (483 to 1600)	87 to 535 (600 to 3690)	250 to 368 (1720 to 2540)
Elastic modulus, x 10 ³ ksi (GPa)	29 (200)	5.1 to 7.4 (35 to 51)	15.9 to 84 (120 to 580)	6 to 18.2 (41 to 125)
Yield strain, %	0.14 to 0.25	N/A	N/A	N/A
Rupture strain, %	6 to 12	1.2 to 3.1	0.5 to 1.7	1.9 to 4.4

The Middle East, and especially the United Arab Emirates, is known for its high temperatures (around 50 °C) and harsh environment, including high humidity during the summer. The use of FRP materials instead of steel reinforcements has many advantages under

these conditions. For instance, FRPs have higher strength, higher corrosion resistance, and a higher strength-to-weight ratio. The lower cost of E-glass FRP compared to other FRP materials makes it a popular reinforcement for concrete. Studying the strength and durability of GFRP materials under the harsh environment found in the Middle East is therefore very important.

1.2. Research Objectives

The main research objectives of this thesis are to:

- Evaluate the GFRP performance after exposure to a harsh environment (high temperature, cycles of seawater splash zone, and high alkalinity) by testing the bond and tensile strengths.
- Predict the long-term performance of GFRP bars using Arrhenius modeling.

Chapter 2: Literature Review

2.1. Bond Strength

Micelli and Nanni [8] tested the mechanical and physical properties of different FRP materials to observe the causes of damage and strength retention. Five types of FRP bars were exposed to alkaline conditions at high temperature. The specimens were also tested under a combination of temperature cycles, high moisture, and ultraviolet radiation.

Properties of the FRP samples used in this study are summarized in Table 2.1. Table

2.1: FRP Rod Properties [8]

Rod	Fibers	Matrix	Diameter (mm)
C1	Carbon	Epoxy/vinyl ester	8.26
C2	Carbon	Epoxy/vinyl ester	8.00
C3	Carbon	Epoxy	7.94
G1 (prototype)	Glass E	Thermoplastic	12.00
G2	Glass E	Polyester	6.35

The time and temperature exposures were: 21 days at 60 °C for exposure 1; 42 days at 60 °C for exposure 2; and, 42 days at 22 °C for exposure 3. The G1 rods had a tensile strength of 924 MPa with a modulus of around 42.6 GPa. The G2 rods showed lower values for their mechanical properties due to their lower fiber content, which made their tensile strength only 326 MPa with a modulus of 30 GPa. The other three rod types were made of carbon fibers. These rods had a high tensile strength, but C3 had a lower tensile strength compared to the other two CFRP rods, which had a tensile strength of 1013 MPa and modulus of 108 GPa.

The ultimate strength decreased noticeably in the G2 rods due to a lower resin. A reduction of 30% was recorded after exposure 1, and 40% after exposure 2. A comparison of the FRP rods made of glass fibers indicated that the thermoplastic resin was better than the polyester resin. The polyester resin was not recommended for the construction industry because it was negatively affected by alkali ion penetration as well.

The research program designed to evaluate the durability performance of FRP reinforcing bars for concrete structures has included the use of accelerated aging tests. Table

2.2 shows lists of materials investigated. GFRP and CFRP bars embedded in concrete were exposed to five different solutions: water, two types of simulated alkaline pore solutions of normal and high performance concrete, saline solution, and an alkaline solution containing chloride ions, as summarized in Table 2.3 [9]. The aging process was accelerated by wetting and drying cycles, as well as freezing and thawing cycles.

Table 2.2: Material Aspects of FRP Specimens [9]

Bar type	Fiber type	Resin type	Bar size	Nominal diameter	Brand name
GFRP1	E-glass	Vinyl ester	#3 and #4	9.53 and 12.70	Aslan 100
GFRP2	E2-glass	Vinyl ester	#3	9.53	N/A
CFRP	Carbon	Epoxy	#3	9.53	Aslan 200

Table 2.3: Compositions of Solution 2 to Solution 5 [9]

Solution no.	Quantity in g/L (mol/L)				
	NaOH	KOH	Ca(OH) ₂	NaCl	Na ₂ SO ₄
Solution 1	Water only				
Solution 2	2.4 (0.06)	19.6 (0.35)	2 (0.027)	-	-
Solution 3	0.6 (0.015)	1.4 (0.025)	0.037 (0.005)	-	-
Solution 4	-	-	-	30	5
Solution 5	-	5.6 (0.1)	-	71.66 (1.23)	-

Two types of concrete mixes were used. The first type was normal weight concrete with strength of 20 MPa, and the second was high performance concrete with a strength of 65 MPa. Pullout tests were conducted to find the effects of exposure on the durability of bond strength between the FRP bars and concrete. Solution 2 was the most damaging environment for the FRP bars. Solution 3 was the next most aggressive, followed by 1 (Water) and then 4. Increasing the temperature of the solutions reduced the strength of the bars. Overall, GFRP bars showed a significant strength loss due to exposure, whereas the strength of CFRP bars did not change significantly; consequently, CFRPs are viewed as more durable than GFRPs under the conditions tested. Continuous immersion of the GFRP bars caused greater strength

loss. GFRP2 had higher tensile strength, despite the similarity of its matrix and manufacturing process to those of GFRP1. This observation indicated that the glass fiber matrix interphase was the cause of reduced durability. The bond strength of FRP bars was also dependent on the type of concrete. Due to its low bond capacity, low performance concrete would split before complete pullout; therefore, the use of high performance concrete with a larger concrete specimen could help to reduce the splitting before pullout.

Robert and Benmokrane [10] studied the durability of the bond between GFRP bars and concrete. They investigated the effect of aging on bonds at different temperatures, and chose GFRP because it is noncorrosive and nonconductive, lightweight, and can provide high strength. The long-term performance of GFRP is very important under special conditions such as highly alkaline environments and high temperatures. The difference in bond strength before and after exposure was considered to be a measure of the durability of the bond between the GFRP bars and concrete. The GFRP bars were embedded in concrete and tested in tap water at 23 °C, 40 °C, and 50 °C.

This previous study used sand-coated GFRP bars with a nominal diameter of 12.7 mm. The 28-day compressive strengths of concrete were between 55 to 62 MPa. A single GFRP bar was embedded along the central axis of the concrete cube, and the bar's bonded length was five times that of the bar diameter. All specimens were cast and kept at saturated humidity for 40 days, and then immersed in tap water at 23 °C for 180 days for initial conditioning. Samples were then exposed to three different temperatures for three different durations (60, 120, and 180 days). Elongation of the bars was recorded during the pullout test using LVDT. The load was applied on the GFRP bar at a rate of 20 kN/min. All the specimens tested under pullout tests failed by slipping through the free-end, and no yielding occurred because of the brittleness of the GFRP material. The bar core pulled out, and bond failure occurred at the interface of the concrete and sand coating or at the interface of the sand coating and the bar. Failure occurred at those sites because of the concrete's high shear strength. Microstructural examination showed no significant interface failure after conditioning of 180 days in 23 °C and 50 °C tap water. The bond strength of GFRP bars therefore appeared to decrease as the duration of immersion increased; however, increasing the temperature up to 50 °C had no major effect on the bond strength. The values of the bond strength retentions were 94%, 93%, and 92% for immersion in tap water at temperatures of 23, 40, and 50 °C,

respectively, after 180 days of exposure. Figure 2.1 shows that the reduction in bond strength is negligible when the temperature is increased to 50 °C.

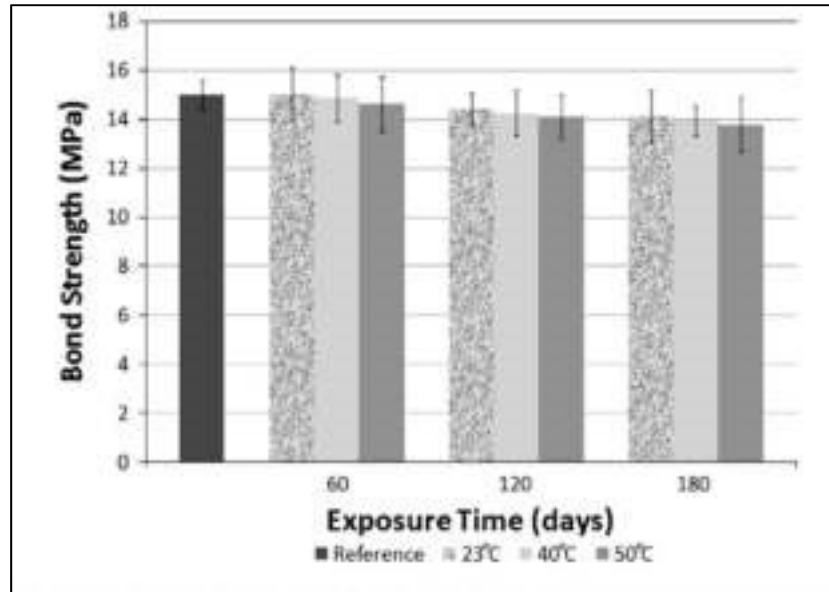


Figure 2.1: Bond-Strength Evolution of Conditioned GFRP Bars at 23 °C, 40 °C, and 50 °C [10]

The effects of temperature and environment on the properties of glass fiber bars have also been examined [11]. The effect of water and alkaline environments on the bond strength was tested under different temperatures ranging from 20 °C to 120 °C. Table 2.4 and Figure 2.4 show the characteristics of the different bars used in this experiment.

Table 2.4: Characteristics of the GFRP Bars Used in the Study, (Manufacturer’s Data) [11]

GFRP rod	Diameter (mm)	Shape	Tensile Strength (MPa)	Elastic modulus (MPa)
G1	12.7	Round	655	40,800
G2	12.7	Round	655	40,800
G3	12.7	Round	800	42,000

The G1 rod has a unidirectional E-glass fiber core with a high-grade polyester resin and sand coating. The G2 was similar to the G1 except that it had a matrix of vinyl ester resin. The G3 bar was made from a continuous E-glass fiber with a matrix of urethanemodified vinyl ester.

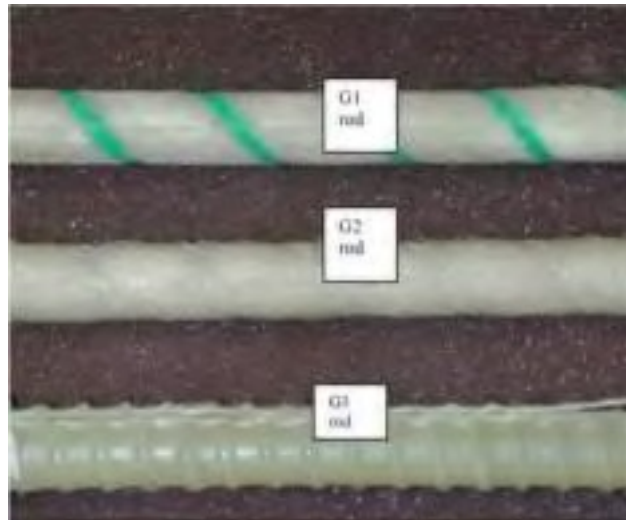


Figure 2.2: Types of GFRP Bars Used in the Experiment [11]

A pullout test was carried out to find the bond strength between the concrete and rebar. Displacement of the machine was controlled at 1 mm/min and different temperatures were examined by using thermocouples at the center of the rod. The effects of environmental exposure to an alkaline situation were tested by immersing the specimens in a liquid containing 1 mol/l NaOH, pH 13. Penetration of the liquid from both ends of the samples was prevented by coating the specimens in an epoxy resin. The bond strength of the bars increased with time; which may reflect an increase in concrete strength over time. Continuing the curing process may lead to a major increase in concrete strength for periods up to a few years [12]. However, the properties of the bars deteriorated when exposed to high temperatures and alkaline environments. Another conclusion from this experiment was that the rate of degradation of the rebar was directly proportional to the nature of the resin matrix.

Zhou et al. [13] used accelerated aging methods to study the long-term bond performance of GFRP bars embedded in concrete to their nearest real value. They chose 120 specimens for bond testing because de-bonding is the most critical mode of failure and weakens the structure. In their experiment, pullout tests were carried out because of their simplicity in determining bond strength. They used GFRP-ribbed bars, with a nominal diameter of 17 mm, made of 28% thermosetting polyester resin and 72% type E glass fibers. The temperature was controlled at 20 °C, and the specimens were tested after 30, 45, 60, and 75 days. The following five different environments were chosen to simulate the real conditions.

(1) Tap water (H₂O), with high humidity;

- (2) Chloride (HCl) + sulfate (H₂SO₄), pH 2;
- (3) Chloride (HCl) + sulfate (H₂SO₄), pH 3;
- (4) Chloride (HCl) + sulfate (H₂SO₄) with a pH 4;
- (5) Specimens open to an indoor natural environment as a control condition.

The maximum bond strength loss occurred after 75 days under the combined exposure to Chloride and Sulfate at pH 2. The researchers concluded that strength of GFRP at pH 2 should be used as a reference in Arrhenius equation because it is the most critical type of environment out of the 5 types in the experiment. The average pH value of acid rain in their region is 5.6. The time to reach a given bond strength retention at different pH values can be approximately calculated by combining results for different environments and plotting bond strength retention vs. the logarithm of time. Arrhenius and time shift factor equations showed that GFRP bars held at pH 5.6 for 232 days responded similarly to being placed in outdoor conditions for 34 years. This means that in places with acid rain, the GFRP embedded in the concrete will lose bond strength quickly. Knowing the durability and bond strength of GFRPs after several years is very important because de-bonding causes structures to fail earlier than expected.

Masmoudi et al. [14] used eighty specimens to study the effect of long-term bond performance of GFRP bars under different temperatures (20, 40, 60, and 80 °C). Pullout bond testing was performed on specimens that had a 500 mm long GFRP bar embedded vertically in 150x150x150 mm and 180x180x180 mm concrete cubes, for 8 and 16 mm bar diameters, respectively. After the thermal treatment (40, 60, and 80 °C) for 4 and 8 months, pullout tests were performed at a displacement rate of 1.2 mm/min. Four LVDTs, with accuracy equal to 0.001 mm, were also attached for each pullout test [14]. The GFRP bars experienced minimal bond strength reduction after 4 and 8 months of exposure at temperatures up to 60 °C. In addition, no major damage was observed on the interface between the GFRP bars and the concrete after 240 days of thermal loading in a dry environment. However, the bond strength decreased as the diameter increased.

Table 2.5 shows a summary of the bond strength of GFRP bars exposed to different solutions for different periods, as presented in various studies.

Table 2.5: Bond strength of GFRP Bars Exposed to Different Solutions in Various Studies

Reference	Matrix material	Diameter (mm)	Exposure type	Temperature	Exposure days	Strength loss (%)
Robert and Nanni [10]	Sand coated	12.7	Water	23	60, 120, 180	0, 4, 6
				40	60, 120, 180	1, 5, 7
				50	60, 120, 180	2, 6, 8
Abbasi and Hogg [11]	E-glass	12.7	Water	60	30, 120, 240	6, 7, 9
			Alkaline (pH 12.5)	39	30, 120, 240	7, 14, 12
Zhou et al. [5]	E-glass Polyester	16	Alkaline (pH 2)	-	30, 45, 60, 75	10, 18, 17, 22
			Alkaline (pH 3)	-	30, 45, 60, 75	9, 10, 14, 16
			Alkaline (pH 4)	-	30, 45, 60, 75	6, 4, 12, 14
Masmoudi et al. [14]	E-glass	16	High Temperature	40	120	2.2
				60	120	3.5
				80	120	4.2

2.2. Tensile Strength

Kim et al. [15] studied the short-term durability of GFRP rods exposed to different environments, including moisture, chloride, alkali with high pH, and freeze-thaw cycling for different periods of time. E-glass/vinyl ester rods 12.7 mm in diameter were used for a tensile test. The impact of harsh environments on the GFRP bars was evaluated by comparing the tensile strength of the exposed bars to that of unconditioned bars. Tap water was used to simulate high moisture. NaCl solution was used to simulate the chloride environment or seawater salinity. KOH, NaOH, and Ca(OH)₂ solutions were used to create alkaline conditions at pH 12.7. Samples were kept in a long galvanized steel tube 50 mm in diameter that was filled with each simulation solution. The tensile strength was reduced in all environments as exposure time increased. The alkali attack damaged the bars more than the other cases; this could be due to a weak interface between the fiber and the matrix.

Porter and Barnes [16] conducted an accelerated test on three different types of GFRP bars in alkaline solutions with high pH at a high temperature of 60 °C for 19-81 days. All bars had a diameter of 9.4 mm and were made of different E-glass resins. Their tensile tests indicated a 29-66% loss in strength. High tensile loss occurred due to the resins used to form the GFRP bars.

Gaona [17] also examined the durability of GFRP bars exposed to alkaline solution. The GFRP rebar was type E-glass/vinyl ester matrix with a diameter of 16 mm. The

temperature was 35 degrees—that is, close to concrete temperature while hardening. Bars were exposed to a high pH for 350 days and showed a tensile reduction of 23%. However, the elastic modulus of the bars increased by 9% over the 50-week conditioning.

Chu et al. [18] studied the effects of alkalinity on the tensile properties of E-glass/vinyl ester composite strips. Specimens were placed into deionized water or alkaline solution at different temperatures (23, 40, 60, and 80 °C) for 18 months. Bars were immersed in alkaline solutions formed by mixing 10.89 g/l of CaCO₃ and 5.95 g/l of Ca(OH)₂ to provide a pH of 11.5, and to simulate concrete pore water. The tensile strength losses were between 35% and 72% of the initial strength.

Al-Zahrani [19] studied the effects of harsh environments on the tensile strength of GFRP bars with different matrix resins. All GFRP bars were type E glass and the resin materials were vinyl ester, modified vinyl ester, and polyurethane. Samples were tested in four aggressive solutions (alkaline, alkaline + seawater, alkaline + sea salt, and acidic) at three different temperatures (60 °C, 24-hour thermal variations of 22 °C and 60 °C, and outdoors) for 3, 6, 9, and 12 months. The tensile test showed the highest percentage reduction for the three types of GFRP bars with exposure to alkaline + sea salt treatment at 60 °C. The GFRP bar with polyurethane was less affected compared to the other types of GFRP bars.

The residual tensile strength of GFRP bare bars has also been examined after subjecting the bars to different environmental conditions for 6 months [20]. The different environments were tap water, seawater, and alkaline solution at different temperatures (23, 35, 50, and 65 °C). The GFRP bars were E-glass type with three layers of urethane-modified vinyl ester that contained 70% fibers. The bars had a diameter of 9.5 mm and a tensile strength of 756 MPa. The reduction in the tensile strength after 6 months was 2.7%, 12%, and 13.7% in the water, seawater, and alkaline solution, respectively.

In North America, bridge deck slabs are exposed to severe environmental conditions such as freeze-thaw action or traffic fatigue loads. The use of GFRP reinforced bars is reasonable; nevertheless, their durability needs more research because information is not documented well in this category. Alves et al. [4] examined the effect of different harsh environments on the bond strength of GFRP bars reinforced in concrete. A total of 36 specimens were tested in a pullout test to investigate the bond strength between the GFRP bars and concrete. To do this test, the specimens were cut in half. The concrete used for this

study was normal concrete with a compressive strength of 50MPa. Different modes of failure were observed in this study:

- Pure pullout failure, where the bar was pulled out of the specimen without cracks or splits.
- Concrete cover failure, where a small crack appeared in the cover and went through the whole block.
- Diagonal failure, which might have occurred because the concrete was not homogeneous.

The fatigue load due to cyclic load caused around 50% of the loss of bonding. Thus, the use of large concrete covers is beneficial when the GFRP bar has a large diameter.

The manufacture of nano-GFRP bars is a recent development. These bars are produced by a pultrusion method like normal GFRP bars; however, during pultrusion, nano materials like silica (SiO_2), alumina (Al_2O_3), and silicon nitride (Si_3N_4) are added to the vinyl ester resin at 1, 3, and 5 percent of the weight. The tensile strength of these new materials is higher than that of normal bars following exposure to alkaline solutions [21]. Table 2.6 shows a summary of the tensile strengths of GFRP bars exposed to different solutions for different durations, as presented in various studies.

The use of high performance concrete is recommended for bond strength because normal weight concrete has low bond capacity that leads to splitting before complete pullout [9]. Therefore, a concrete with 50MPa compressive strength is used in the current study. Different studies show that a GFRP bar containing vinyl ester resin is better than one containing a thermoplastic or polyester resin [8,11]. Therefore, the GFRP bars selected for the current study contained vinyl ester resin. The bond and tensile strength reductions were also expected to be less for bars exposed to high temperature than for bars exposed to alkaline conditions.

In the current study, GFRP bars were directly exposed to harsh environments, unlike the cases in the previous studies where bars were either embedded in concrete for pullout tests or covered by cement mortar for tensile tests. Kim et al. [15] also exposed GFRP bars directly to harsh environments prior to a tensile test. This scenario, where bars are directly exposed, can happen in real life applications; for example, when bars are in storage before delivery to the construction site or when bars are delivered to the site and the project is

delayed for some reason. Table 2.6 shows the tensile strength of GFRP bars exposed to different solutions for different periods of time in various studies.

Table 2.6: Tensile Strength of GFRP Bars Exposed to Different Solutions in Various Studies

Reference	Matrix glass material	Bar diameter (mm)	Conditioning solution	Temperature	Exposure period (days)	Tensile loss (%)
Kim et al [15]	E-glass/vinyl ester	12.7	Water	25, 40, 80	132	11, 16, 22
			Sea water	25, 40, 80	132	14, 13, 19
			Alkaline (pH 13)	25, 40, 80	60	32, 30, 40
Porter & Barnes [16]	E-glass/IP, BV	9.4	Alkaline	60	19-81	29-66
Gaona [17]	E-glass/vinyl ester	16	Alkaline (pH 12)	35	350	23
Chu et al. [18]	E-glass/vinyl ester	Strip:0.063x 15.24	Deionized water	23, 40, 60, 80	525	35, 49, 63, 72
			Alkaline			42, 47, 61, 62
Al-Zahrani [19]	E-glass/modified vinyl ester	12	Alkaline (pH 13.5)	60	360	77
			Alkaline + sea water	60		58
			Alkaline + Sabkha	60		49
			Thermal variation	20 to 60		5
			Outdoor	Varied		6
Al-Zahrani [19]	E-glass/vinyl ester	12	Alkaline (pH 13.5)	60	360	71
			Alkaline + sea water			77
			Alkaline + Sabkha			66
Al-Zahrani [19]	E-glass polyurethane	12	Alkaline (pH 13.5)	60	360	21
			Alkaline + sea water	60		19
			Alkaline + sea salt	60		27
			Thermal variation	22-60		15
			Outdoors	Varied		21
Alsayed et al. [20]	E-glass/urethane Modified vinyl ester	9.5	Water	50	180	2.7
			Sea water			12
			Alkali solution			13.7
Chen et al. [22]	E-glass/vinyl ester	9.5	Water	20, 40, 60	120 for 20	5, 3, 29
			Alkaline (pH 13.6)			14, 11, 36
			Alkaline (pH 12.7)		70 for 40 and 60	8, 8, 27
			Sea water			3, 2, 26
Chen et al. [22]	E2-glass/vinyl ester	9.5	Alkaline (pH 13.6)	40, 60	60	31, 48
				20	120	45

Chapter 3: Material and Environment Preparations

3.1. Concrete Wooden Forms

A total of 20 cubic wooden forms required for the pullout tests were manufactured to test the bond strength of GFRP bars embedded in concrete. Each side of a cube form was 200 mm thick, with a small 16 mm diameter hole cut into the bottom center at a depth of 10 mm. Figure 3.1 shows samples of the prepared wooden forms before casting the concrete.



Figure 3.1: Samples of Cubical Wooden Forms Prepared for the Pullout Test

3.2. GFRP Bars

A total length of 30 meters of GFRP bars was used for both the pullout and tensile tests: 20 meters of 16mm diameter bar for the pullout test, and 10 meters of 12 mm diameter for the tensile test. The maximum length of the GFRP bars for each sample was 1 meter; therefore, to simplify the exposure, each bar was cut to 1 meter length before being put into different exposure environments. The bars were coated with an epoxy resin on both ends to prevent penetration of liquid. Figure 3.2 shows the GFRP bars before exposure.



Figure 3.2: GFRP Bars before Exposure

3.3. Splash Zone Exposure

A sustainability center was designed for the project in order to simulate the splash zone in a harsh environment. Samples were placed in the lower tank containing 4% saline water. A water pump was used to move the water to the upper tank. Water then returned to the lower tank via gravity. This environment creates wet/dry cycles of saline water for samples in the tank, which is more severe than simply exposing the bars to saline solution without wet/dry cycles, as was done in previous studies. Figure 3.3 shows the sustainability center and the bars inside the tank.



Figure 3.3: AUS Sustainability Center for Simulating the Splash Zone

3.4. Alkaline Solution Exposure

Sodium hydroxide (NaOH) is a strong base that is highly soluble in water. Thus, laboratory sodium hydroxide pellets were used to provide an alkaline environment with a pH of 13. To reach the desired pH value, 0.1 mole of NaOH was needed per liter of water. Since NaOH has a molar mass of 40 g/mol, 4 grams of NaOH should be dissolved in 1 liter of water to obtain pH 13. Figure 3.4 shows the GFRP bars exposed to the alkaline environment, and Figure 3.5 shows laboratory grade sodium hydroxide pellets.



Figure 3.4: GFRP Bars Exposed to the Alkaline Environment



Figure 3.5: Laboratory Grade Sodium Hydroxide Pellets

3.5. High Temperature and Humidity Exposure

The last exposure type was the high temperature and humidity environment. The GFRP samples were simply placed on the ground next to the sustainability center during the summer, when the temperature was at its highest. Figures 3.6 and 3.7 show the variations in temperature and humidity recorded during the GFRP bar exposure, respectively. Daily temperatures and humidity percentages are presented in Appendix A.

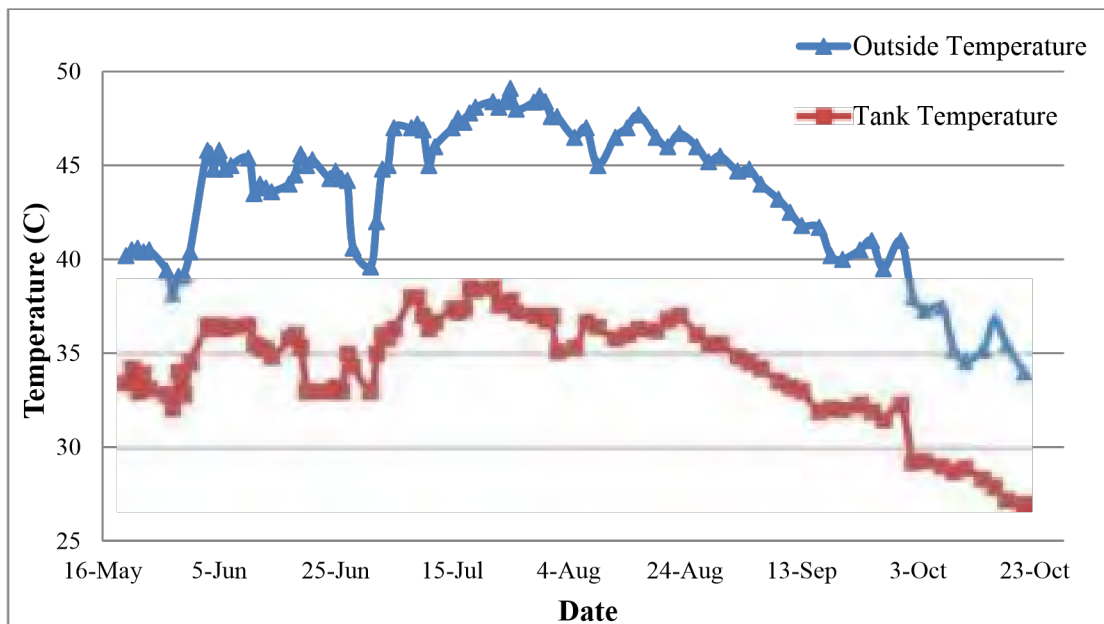


Figure 3.6: Variations in Temperature during the Exposure of Bars

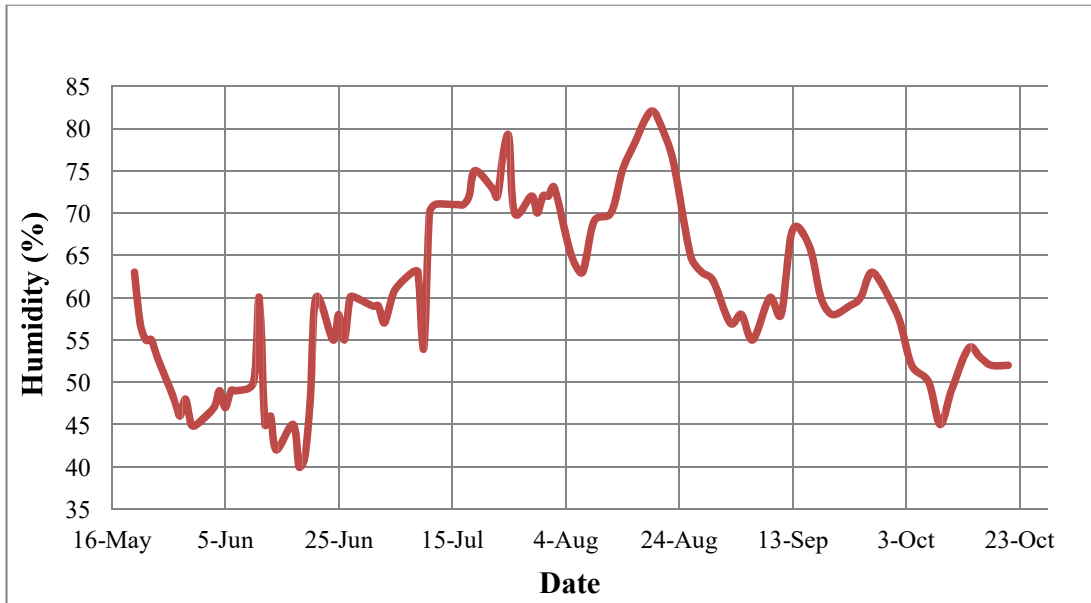


Figure 3.7: Variations in Humidity during the Exposure of Bars

Chapter 4: Research Methodology

4.1. Characteristics of the Materials

4.1.1. Concrete

The concrete mix design used for the pullout samples in this study had a compressive strength of 50 MPa. The concrete was mixed and cast by a local company, Conmix Company. The mix design information and details are provided in Tables 4.1-4.2.

Table 4.1: Concrete Mix Design Specifications (Conmix Company)

Concrete Mix Design					
Strength Class	C50				
Cube Comp. Str.	50 MPa @ 28 Days				
Max Agg. Size	20 mm				
Cement Qty	450 (Kg/m ³)				
Cement Type	OPC				
Water/Cement	0.38				
Aggregate	0/0.6mm	0/5 mm	0/5 mm	5/10 mm	10/20 mm
Source	Al Ain	Siji	RAK	Siji	Siji
Moisture %	0.8	1.2	1.5	0.3	0.3
Absorption %	0.8	1.2	1.5	0.7	0.7
Specific Gravity	2.6	2.7	2.6	2.9	2.9
Percent Mix	13	35	0	18	34

Table 4.2: Concrete Mix Design Detailed Specifications (Conmix Company)

Material	Volume (L)	Specific Gravity	Proportions (kg/m ³)	Absorption %	Moisture %	Moisture correction (kg/m ³)	Final proportion (kg/m ³)
Cement	145.16	3.1	450	0	0	-	450
GGBS	0	2.9	0	0	0	0	0
Micro Silica	0	2.2	0	0	0	0	0

Water	171	1	171	0	0	-0.5	171
Washed Sand 0/5 mm	231.91	2.7	626	1.2	1.2	0	630
Red Dune sand 0/0.6 mm	86.14	2.6	224	0.8	0.8	0	220
CR Sand (0/5) mm	0	2.6	0	1.5	1.5	0	0
CR Agg. 10/20 mm	225.28	2.9	662.3	0.7	0.3	-2.6	660
CR. Agg. 5/10 mm	119.27	2.9	350.6	0.7	0.3	-1.4	350
Additive1	6.25	1.21	7.56	0	60	4.5	7.56
Additive2	0	1.20	0	0	60	0	0
Additive3	0	1.20	0	0	60	0	0
Air	15	-	-	-	-	-	-
	1000						2489

4.1.2. GFRP

The mechanical and physical properties of the GFRP bar used in this study are summarized in Table 4.3.

Table 4.3: Mechanical and Physical Properties of GFRP Bar

Material Property	Units	Value
<i>Mechanical Properties</i>		
Tensile strength	MPa	1000
Tensile modulus	GPa	54.5
Shear strength (single sided)	MPa	260
Shear strength (double sided)	MPa	520
<i>Physical properties</i>		

Longitudinal coefficient of thermal expansion	$\times 10^{-6}/C$	7.2
Transverse coefficient of thermal expansion	$\times 10^{-6}/C$	22
Moisture absorption	%	0.024
Glass content	% Volume	65.4
	% Weight	75

4.1.3. Epoxy

Finding the best applicable epoxy is one of the critical points for the pullout test because the GFRP bar should be completely attached to the grip, and slippage should not occur in the grip between the epoxy and the bar. Concrecive 1450i, manufactured by the BASF Company, was the most suitable epoxy for the pullout test. It contains two components of advanced pure epoxy in side-by-side cartridges. It is more convenient to use the special shotgun when applying the epoxy to the desired area, and it helps the contents of the two cartridges to mix well. Table 4.4 shows the setting time of the epoxy and Figure 4.1 shows a sample of the Concrecive 1450i.

Table 4.4: Setting Time of the Concrecive 1450i

Temperature (°C)	Working Time (minute)	Curing Time (minute)
-5	120	420
0	60	240
5	20	120
20	7	30
30	4	25
40	2	15



Figure 4.1: Concrecive 1450i Container

Generally, the use of GFRP bars is expected to improve the durability of the structure compared to normal steel reinforcements because of the resistance to corrosion of the GFRP bars. However, the properties of the materials can change under high temperatures and highly alkaline environments, so different tests should be conducted to study the behavior of the GFRP bars following exposure to harsh environments. Investigating the bond and tensile strength is the main objective of the present study. Table 4.5 shows numbers of specimens and the duration of the exposure for the GFRP bars used in the present study.

Table 4.5: Number of Specimens and Duration of the Exposure

Exposure to sun	Exposure to splash zone	Exposure to alkalinity
2 specimens for 30 days	2 specimens for 30 days	2 specimens for 30 days
2 specimens for 60 days	2 specimens for 60 days	2 specimens for 60 days
2 specimens for 90 days	2 specimens for 90 days	2 specimens for 90 days

4.2. Pullout Test

Bond stress is the strength between the interaction of the rebar surface and the concrete surface. The pullout procedure is the main test used to find the bond strength with which the rebar is embedded in the concrete, and a tensile force is applied at a constant rate to pull the GFRP bar out of the concrete [23].

GFRP samples were kept in the specified environment to start the exposure. Wooden forms for the concrete were prepared as per the test geometry recommended by the ACI 440.3R-04 code [24], also shown in Figure 4.2. The GFRP bars were kept in the different environments for 30 days, and then two samples were taken from each exposure, as well as two unconditioned control samples from the lab. A total of 8 wooden forms, and 8 GFRP bars were taken to Conmix Company to cast the concrete. Specimens were 200 mm concrete cubes with a single bar embedded vertically along the central axis of the wooden form, as shown in Figure 4.3. The bar's bonded length (80 mm) was five times the bar diameter. The de-bonding tube should be strong enough to allow complete pullout of the bar from the concrete cube. After testing different materials, Poly Vinyl Chloride (PVC) pipes were chosen as de-bonding tubes to prevent contact between the bar and the concrete. Figure 4.4 shows the samples after concrete casting by the Conmix Company. This procedure was also repeated for 60 and 90 day exposures.

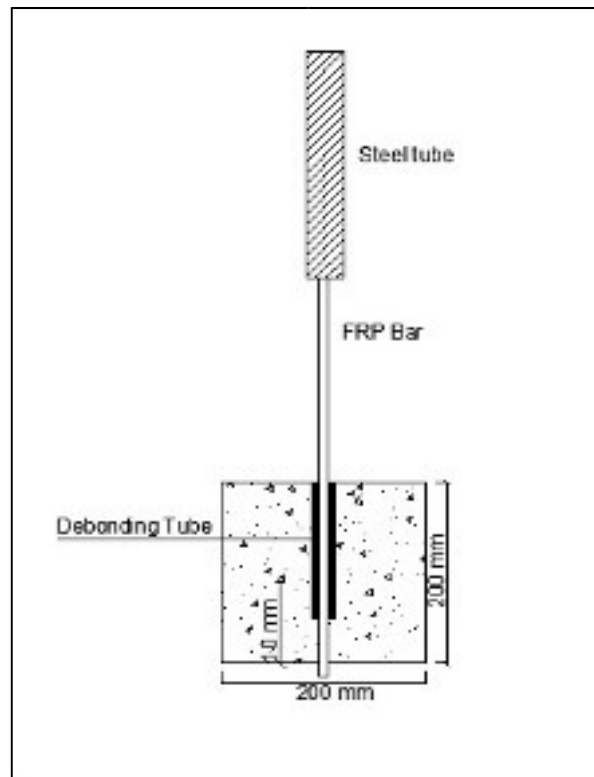


Figure 4.2: Pullout Test Specification [24]



Figure 4.3: Samples of Cubic Wooden Forms Prepared before Casting Concrete



Figure 4.4: Samples after Casting

After initial hardening, samples were returned to the construction material laboratory at American University of Sharjah for curing, in order to reach their maximum compressive strength of 50 MPa. After 28 days of curing, samples were ready for pullout tests.

The steel anchors were designed according to ASTM (D7205/D7205M-06) to grip the GFRP bars during the test. The bond between the bar and grip had to be sufficiently strong that the failure would not occur in the gripping anchor. Concessive 1450i was used as a strong epoxy to attach the bar to the grip. In addition, in the bottom part, a square framed steel plate was used to hold the cube firmly to the machine. All specimens were subjected to a direct pullout test according to ACI 440.3R-04. The test was carried out using a Universal Testing Machine (UTM) of 1200 kN capacity that is available at the American University of Sharjah. The pullout tests were conducted at a loading rate of 10kN/min. The information including the applied load, extension, and bond strength were recorded using an automatic data acquisition system. Figure 4.5 shows the pullout test set up in the laboratory.

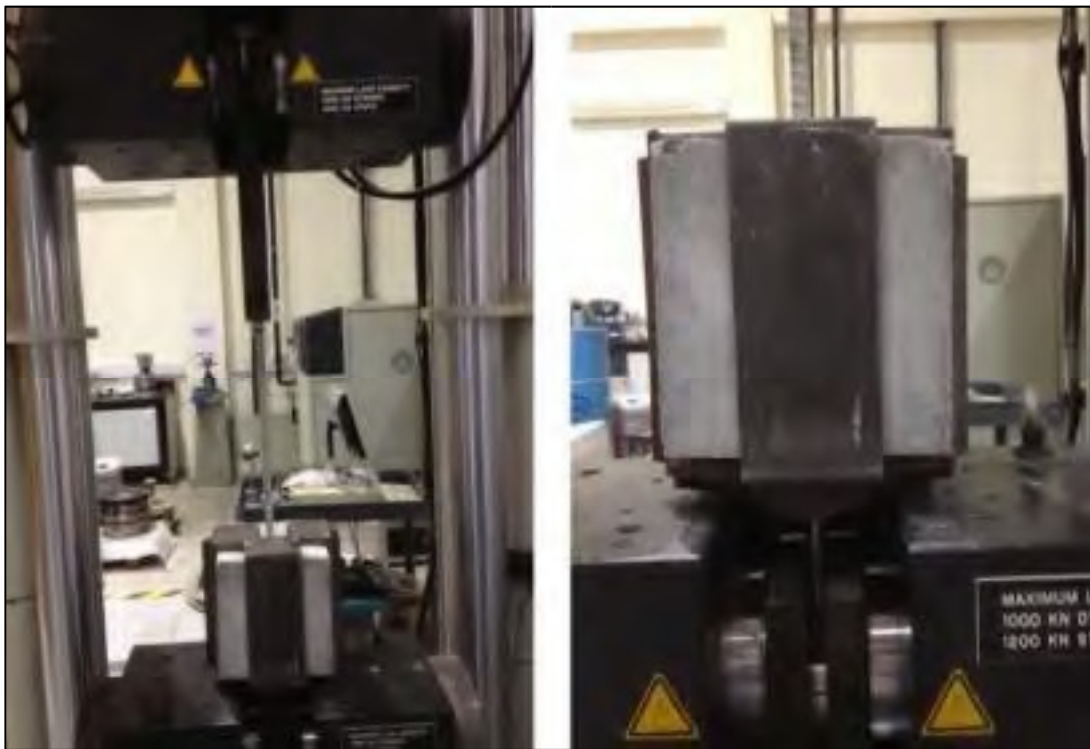


Figure 4.5: Pullout Test Setup

4.3. Tensile Test

The tensile test suggested by the ASTM D638–10 [25], with the geometry shown in Figure 4.6, was utilized in this study to evaluate the tensile strength of GFRP bars. After each time period, two samples were collected from each type of exposure and the bars were prepared and cut for the uniaxial tensile test. Figure 4.7 shows samples of the GFRP bar specimens used for the uniaxial test. The test was carried out using a Universal Testing

Machine. Special steel grips, as shown in Figure 4.8, were needed to grip both ends of the GFRP bars during the test in order to prevent slippage of the bars prior to failure. Figure 4.9 shows the tensile test setup using the UTM.

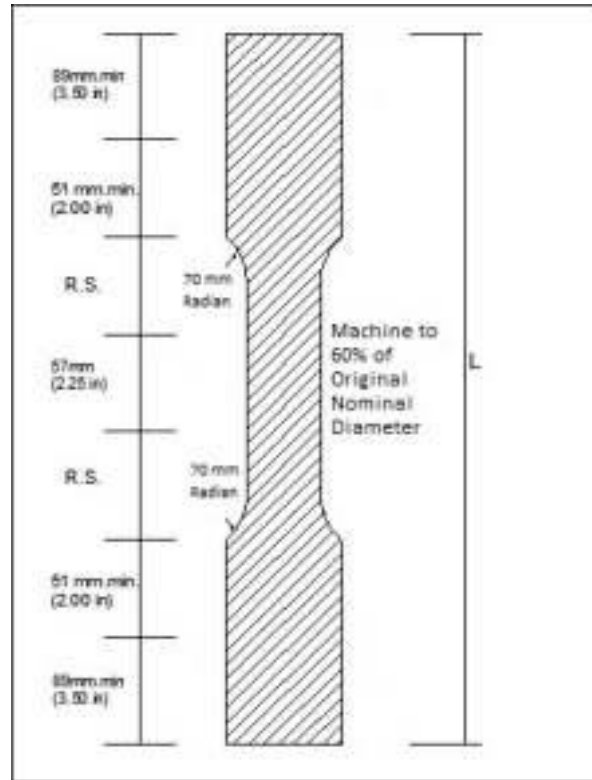


Figure 4.6: ASTM D638–10 Standards for Tensile Test [25]



Figure 4.7: GFRP Bars after Cutting



Figure 4.8: Steel Grips for Gripping Both Ends of GFRP Bars during the Uniaxial Test

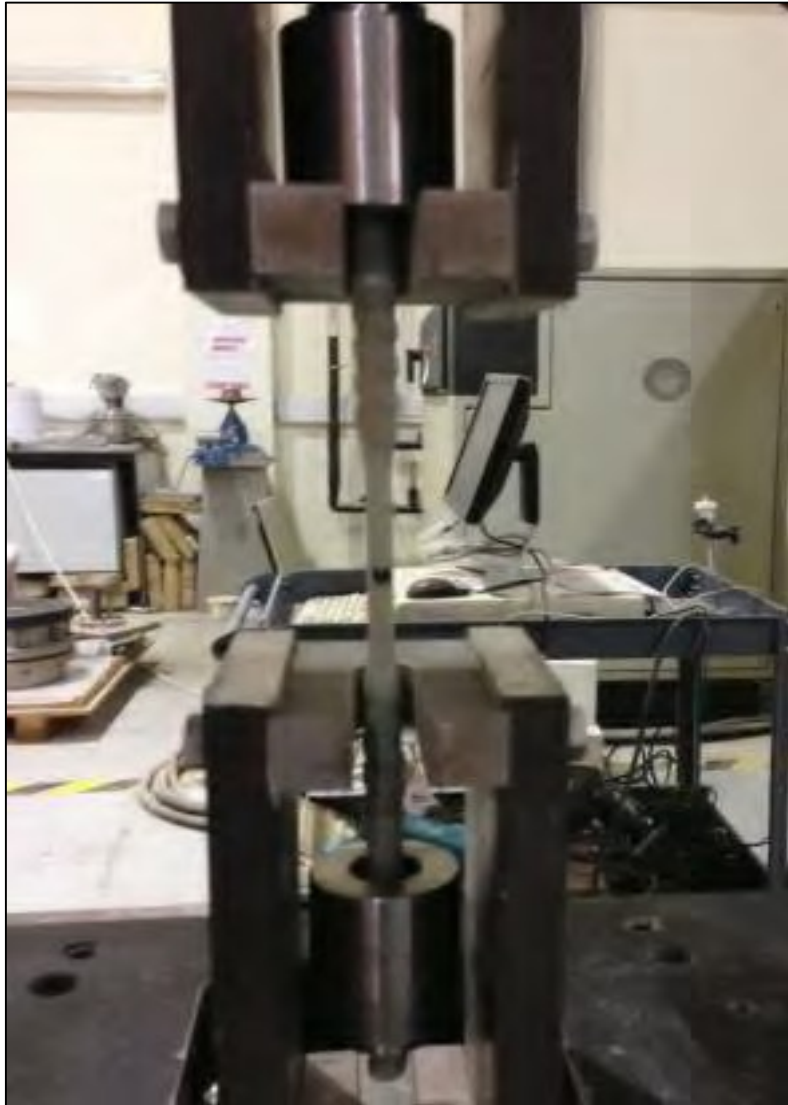


Figure 4.9: GFRP Bar Tensile Test Setup

Chapter 5: Results and Discussion

5.1. Pullout Test

Table 5.1 shows the maximum load for each pullout specimen and its failure mode. The bond strength was calculated using the typical shear equation [11]:

$$T = P/A \quad (5.1)$$

where T is the bond strength, P is the maximum load, and A is the circumferential area of the embedded bar = (The bar's bonded length) x (circumference) = $(5d_b) \times (\pi d_b) = 5\pi d_b^2$.

Table 5.1: Maximum Load, Bond Strength, and Failure Type of the Specimens after Pullout Test

Sample	Maximum Load (kN)	Bond Strength (MPa)	Type of Failure
Lab-1	85.0	21.1	Bar pull out
Lab-2	85.4	21.2	Bar pull out
Sun 30-1	79.3	19.7	Bar pull out + Concrete Block Split
Sun 30-2	83.0	20.6	Bar pull out
Sun 60-2	78.0	19.4	Bar pull out
Sun 60-2	79.8	19.8	Bar pull out + Concrete Cover Failure
Sun 90-1	71.1	17.7	Bar pull out
Sun 90-2	73.8	18.3	Bar pull out + Concrete Cover Failure
Salt 30-1	75.8	18.9	Bar pull out
Salt 30-2	77.9	19.4	Bar pull out + Concrete Cover Failure
Salt 60-1	71.6	17.8	Bar pull out
Salt 60-2	71.9	17.9	Bar pull out
Salt 90-1	68.1	17.0	Bar pull out
Salt 90-2	69.3	17.2	Bar pull out
Alkaline 30-1	70.5	17.5	Bar pull out
Alkaline 30-2	70.6	17.6	Bar pull out + Concrete Block Split
Alkaline 60-1	60.1	15.0	Bar pull out
Alkaline 60-2	60.6	15.1	Bar pull out + Concrete Cover Failure
Alkaline 90-1	50.9	12.7	Bar pull out
Alkaline 90-2	62.3	15.5	Bar pull out + Concrete Cover Failure

All the pullout specimens failed by slipping through the free end. Three failure modes were mainly observed during the pullout tests of the GFRP bars with concrete. The first mode was a complete pullout failure, where the bar was pulled out of the concrete specimen without any splitting or cracking along the concrete surfaces, as shown in Figure 5.1. The second

failure mode was controlled by the failure of the concrete cover, where cracks developed along the concrete surface, as shown in Figure 5.2. On the other hand, a concrete block split was observed as a third type of failure mode, as shown in Figure 5.3. The third failure mode was observed in two samples only: one exposed to sun and the other was exposed to alkaline conditions, both for 30 days of exposure.



Figure 5.1: Complete Pullout Failure



Figure 5.2: Failure of the Concrete Cover

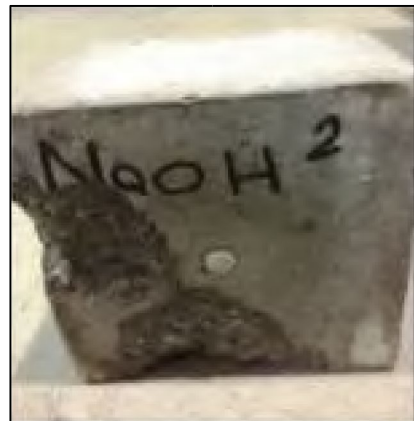


Figure 5.3: Concrete Block Split

Figure 5.4 shows one example of the load-extension relationship of the GFRP bar during the pullout test. After reaching its maximum load, the load drops to zero immediately. The loads vs. extension graphs for all other samples are presented in Appendix B.

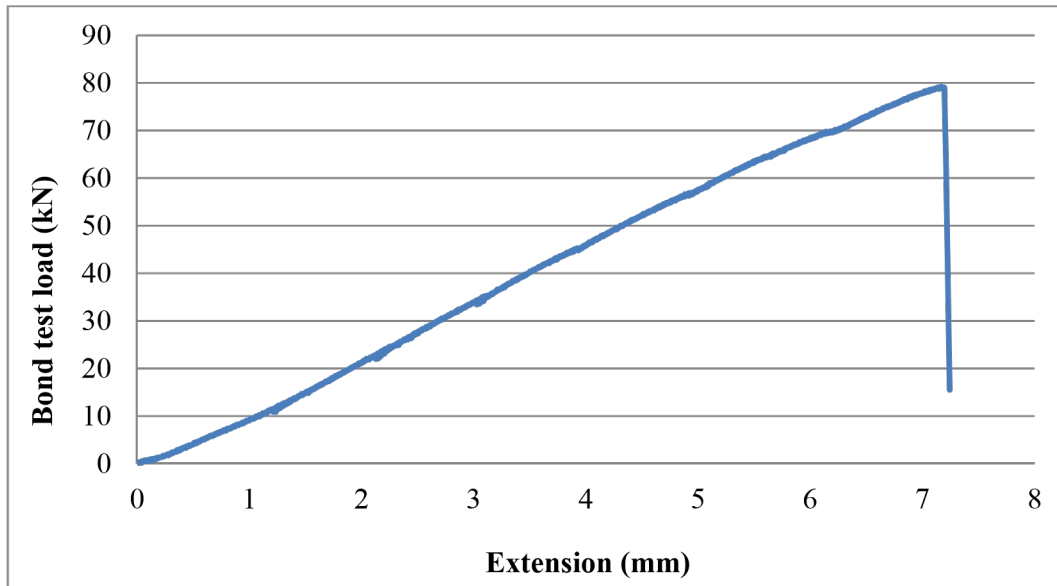


Figure 5.4: Load-Extension Relationship of GFRP Bar Exposed to the Sun after 30 Days

The GFRP bars were directly exposed to solutions known to significantly accelerate aging in order to predict their long-term durability. Figure 5.5 and Figure 5.6 show bar charts of the maximum load and bond strength, respectively, of each specimen in the pullout test. A variation in the effects of each exposure can be clearly seen. High temperature and humidity had the lowest effect on the bars compared to the other two exposures. The bond strength of the GFRP bars that were kept in splash zone exposure had slightly lower values than those kept in the hot and humid exposure. However, the alkalinity effect on the bond strength of GFRP bar was greater than that seen with the other exposures, as the bond strength was significantly lower.

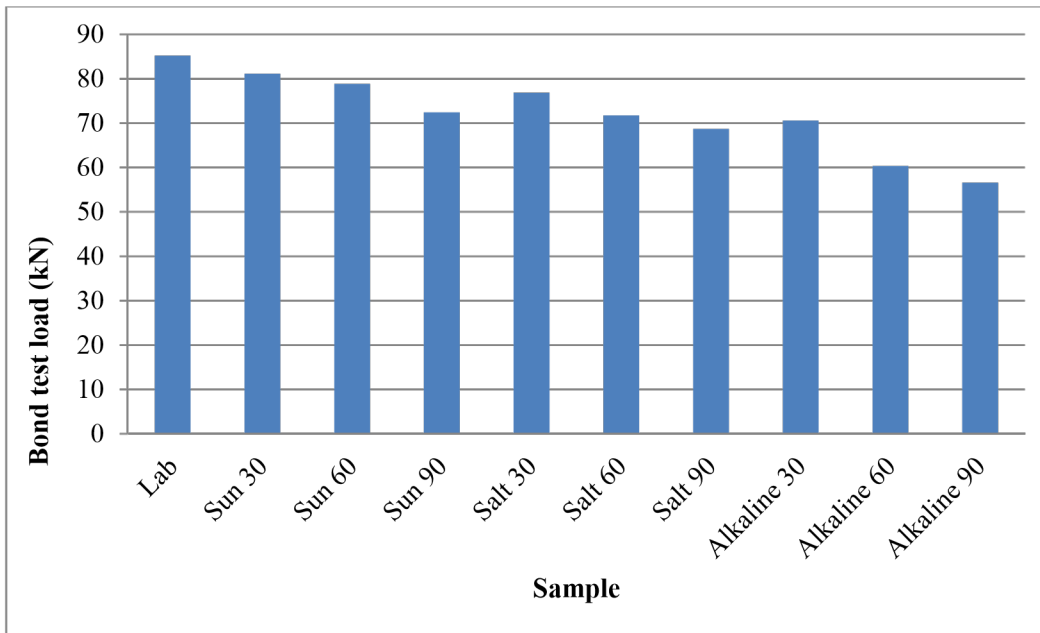


Figure 5.5: Maximum Load for Each Specimen after the Pullout Test

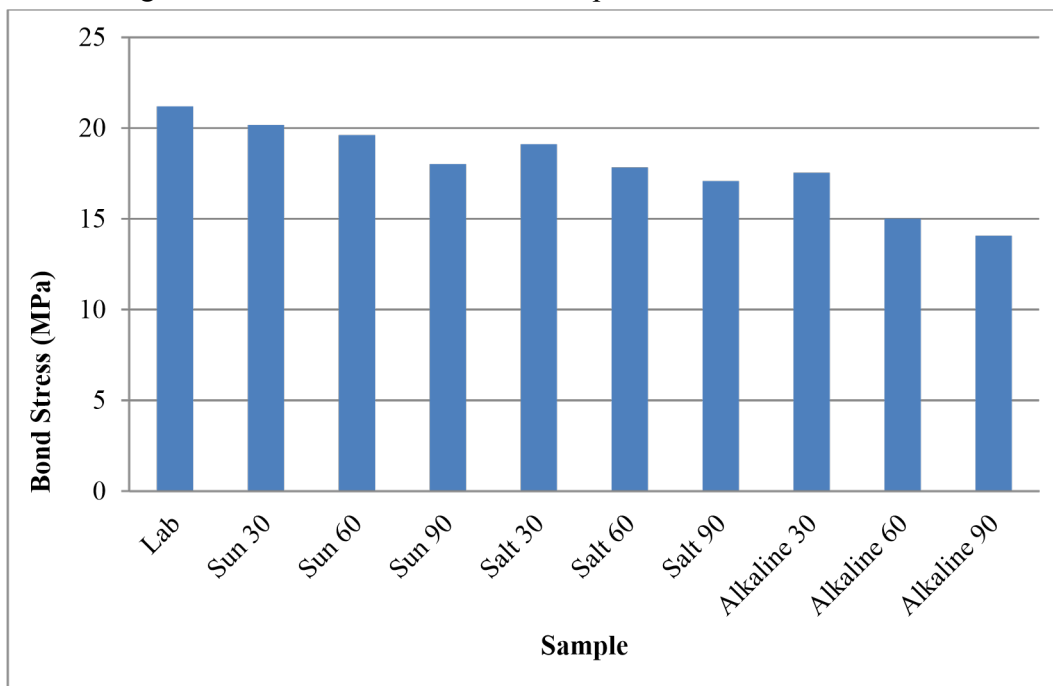


Figure 5.6: Bond Stress for Each Specimen

Figure 5.7 shows the percentage retention for the three different exposures. The alkaline environment clearly has the greatest effect on the GFRP bars. The specimens exposed to the high temperature and humidity showed a high reduction after 90 days of exposure.

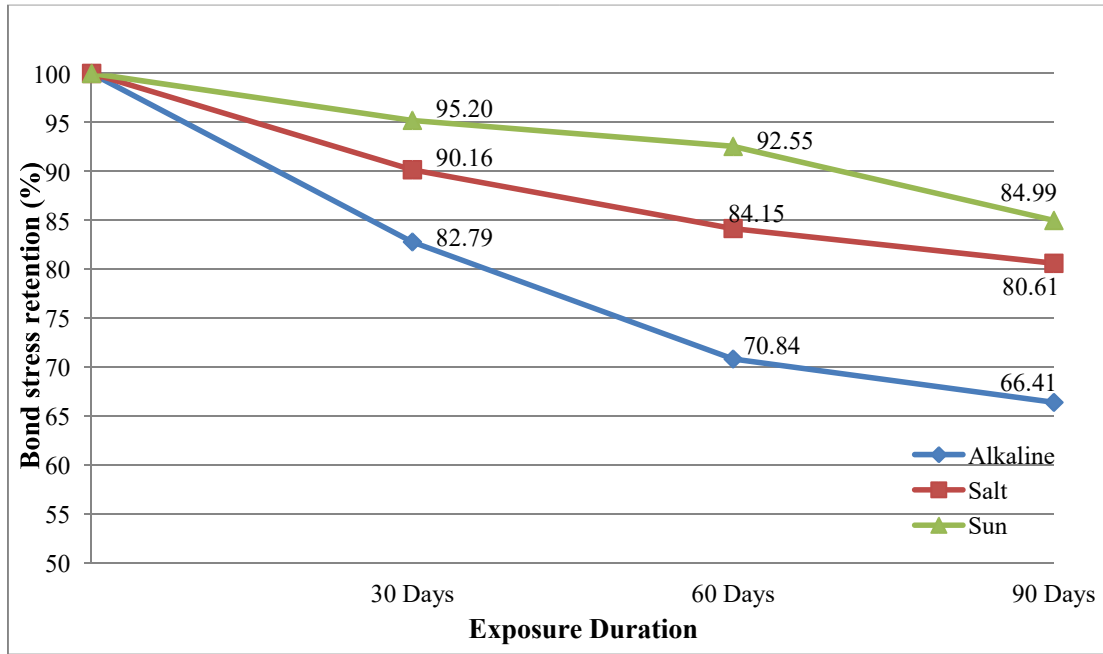


Figure 5.7: Percentage Retention of Bond Stress for Different Type of Exposures

The bond strength of GFRP bars obtained in the present study was also compared with reported results from other studies. Figure 5.8 shows a comparison of the bond strength retention for GFRPs exposed to sun for different durations with results presented by three other authors. The degradation trend of the bond strength observed in current study is generally steeper than that reported in the other studies. This is due to different method of exposure. In the other studies, the bars were exposed to the sun while embedded in the concrete cube, whereas in the current study, the bars were directly exposed to the sun. Previous studies used the same type of exposure, and the differences in their results, as shown in Figure 5.8, arose because Robert and Benmokrane [10] used sand-coated GFRP bars, which have weaker glass fibers.

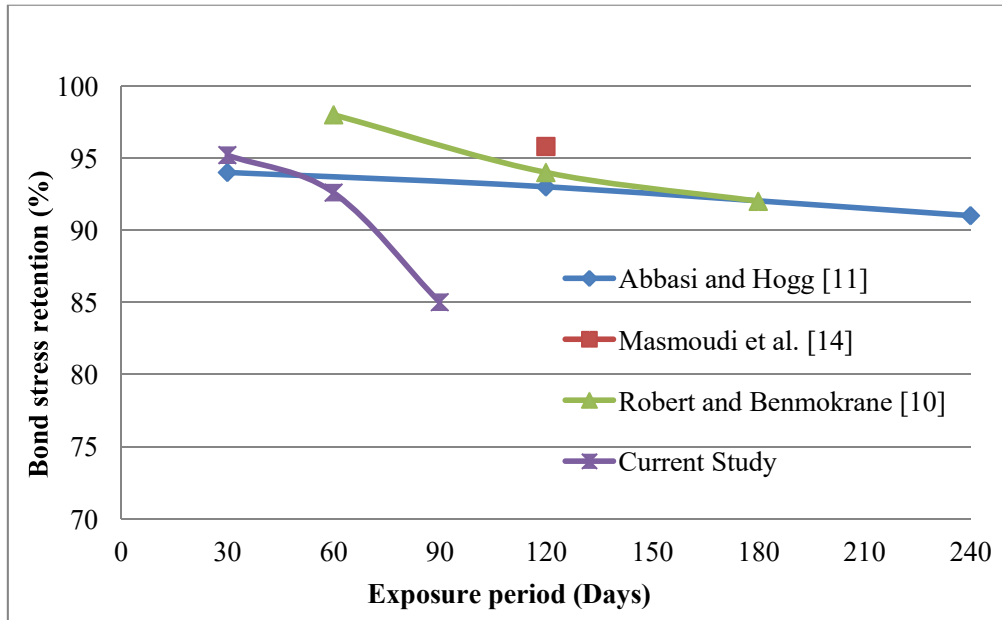


Figure 5.8: Retention of Bond Stress of GFRP Bars Exposed to Sun

5.2. Tensile Test

Uniaxial tensile tests were conducted on GFRP bars after each exposure period. All samples underwent sudden failure due to the brittleness of the GFRP material, and they experienced the same failure mode, which was the separation of glass fibers along the deformed surface, as shown in Figure 5.9.



Figure 5.9: GFRP Bar Mode of Failure after a Tensile Test

Table 5.2 shows a summary of the tensile test results, including the maximum load and tensile strength for each specimen.

Table 5.2: Maximum Load and Tensile Strength Capacity for all GFRP Specimens

Exposures	Duration	Maximum Load (kN)	Tensile Stress (MPa)
Lab-1	-	59.2	950.8
Lab-2	-	60.0	964.2
Sun-1	30	60.0	964.4
Sun-2	30	59.4	954.0
Sun-1	60	57.7	926.9
Sun-2	60	56.9	914.0
Sun-1	90	55.4	889.8
Sun-2	90	55.3	889.2
Salt-1	30	56.4	906.6
Salt-2	30	56.5	909.0
Salt-1	60	55.4	891.1
Salt-2	60	55.2	887.8
Salt-1	90	54.1	869.8
Salt-2	90	49.2	790.5
Alkaline-1	30	55.5	892.0
Alkaline-2	30	56.8	912.3
Alkaline-1	60	58.3	937.3
Alkaline-2	60	58.2	935.5
Alkaline-1	90	59.5	955.7
Alkaline-2	90	58.0	931.9

A sample of the stress-strain relationship for an unconditioned GFRP bar is presented in Figure 5.10. The current study focused on retention of the tensile stress, so strain gauges were not used to record the strain values.

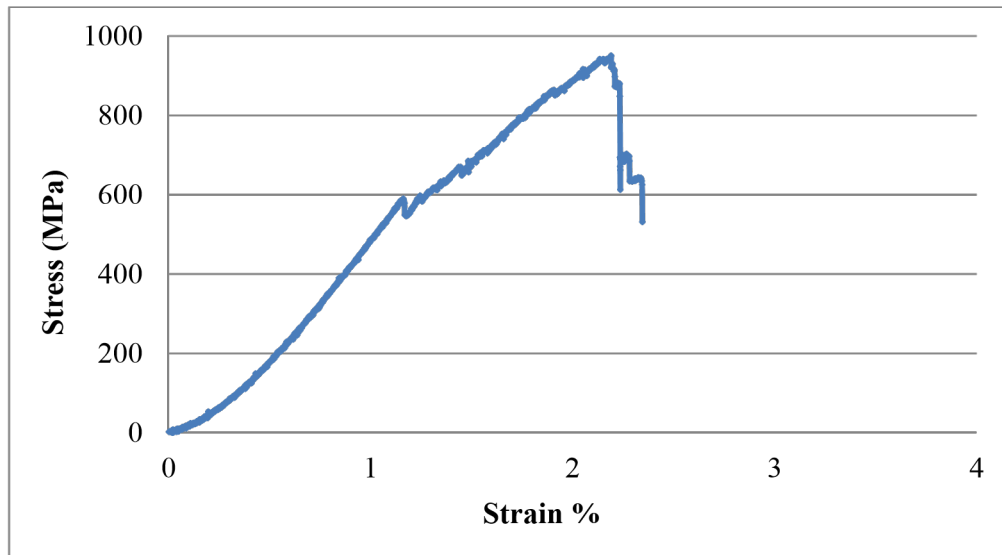


Figure 5.10: Stress-Strain Relationship of Unconditioned GFRP

A comparison of the tensile strength between the control specimen and all other exposures is illustrated by the bar chart shown in Figure 5.11. High temperature and humidity had the least effect on the bars compared to the other two exposures. The tensile strength recorded for the GFRP bars kept in the splash zone exposure was slightly lower than that observed for the GFRP bars exposed to sun, for the three durations. On the other hand, alkalinity exposure had a different effect on the tensile strength of the GFRP bars. The tensile strength decreased after 30 days of exposure, and then increased after 60 days and 90 days of exposure. More investigation is required because no evidence exists for increasing tensile strength of GFRP bars exposed to alkaline environments. A chemical reaction may be occurring between the alkaline solution and the glass material; this reaction may be rapid at the beginning and then needed more time to cause a reduction in the strength of the bars. Figure 5.12 also shows the tensile percentage retention for the three different exposures.

The GFRP specimens exposed to the high temperature and humidity showed no significant reduction after 30, 60, and 90 days of exposure. Figure 5.13 shows a residual tensile strength comparison between the current study and another study that used the same type of exposure. The trend lines of the tensile strength retention for both studies are the same; however, the percentage retention in each study is different over specific days of exposure. Kim et al. [15] found that GFRP bars retained almost 83% of their initial strength after 90 days of exposure. In current study; however, the strength retention was around 93%

for the same period of exposure. This shows that the GFRP bars used in current study had better performance than those used in the previous study.

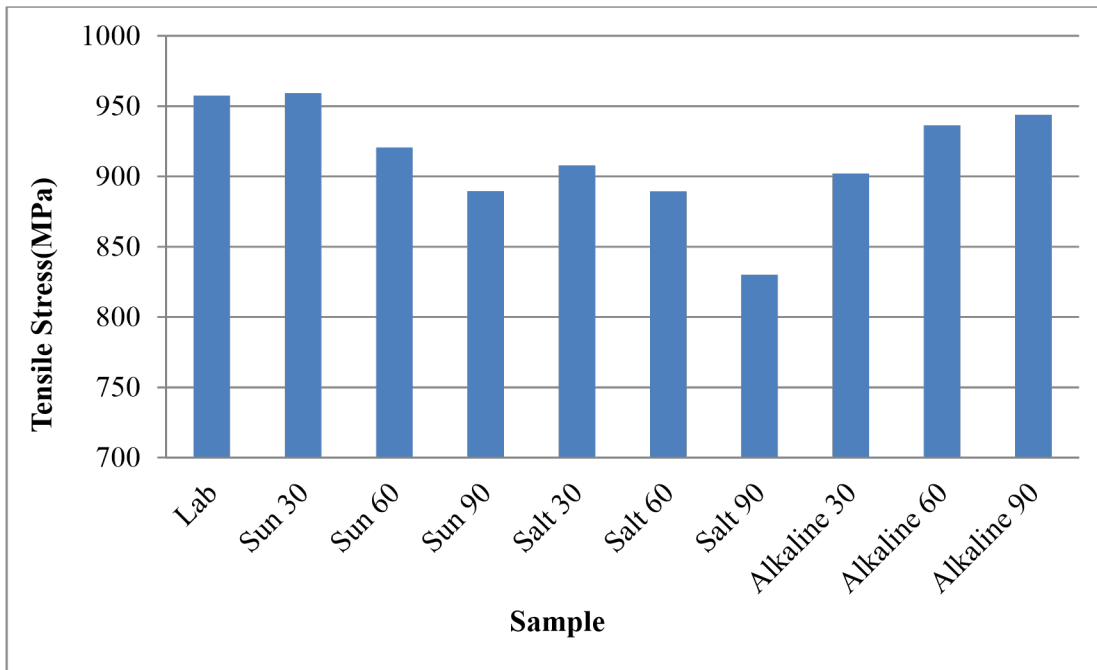


Figure 5.11: Maximum Tensile Stress for Different Types of Exposures

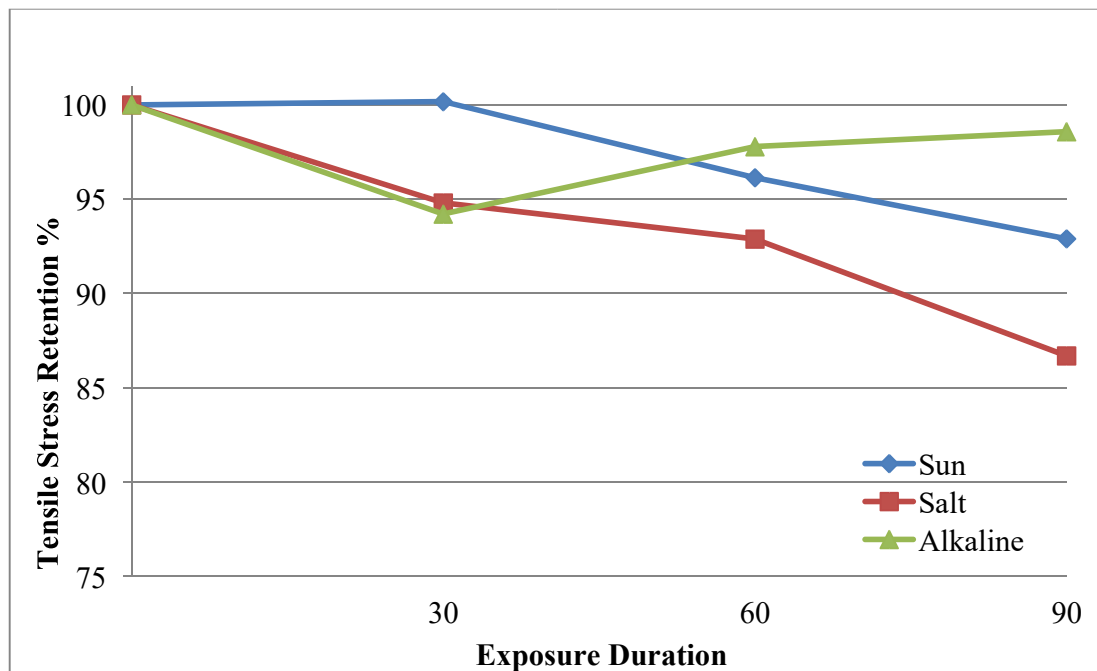


Figure 5.12: Percentage Retention of Tensile Stress for Different Types of Exposures in Current Study

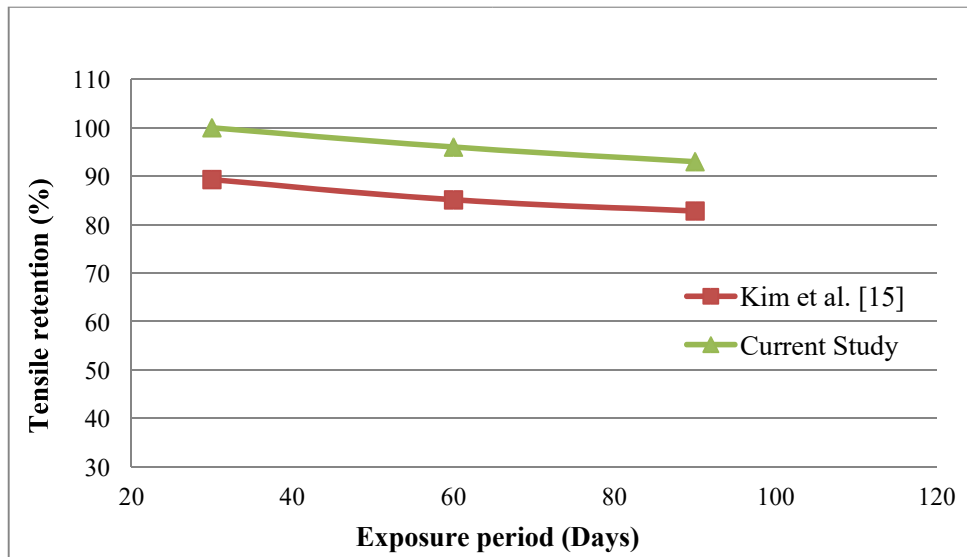


Figure 5.13: Retention of Tensile Strength of GFRP Bars Exposed to Sun Compared to Previous Study

For the specimens exposed to the seawater simulation tank, the strength loss was 13% after 90 days of exposure in the current study and 16% in a previous study, as shown in Figure 5.14. The trend lines are not the same because other factors affected the exposure. In the current study, the seawater environment was simulated in tanks with wet/dry cycles open to air, so the high temperature also contributed to the degradation of the tensile strength of the GFRP bars. Although the current study had a more severe environment, the bars showed better performance after 90 days of exposure to saline solution.

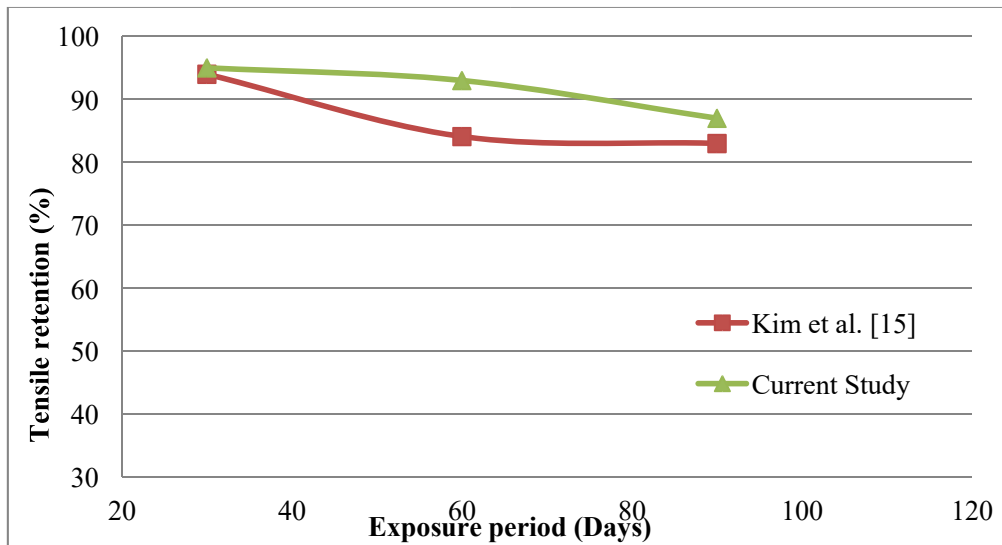


Figure 5.14: Retention of Tensile Strength of GFRP Bars Exposed to Seawater Solution Compared to Previous Study

A comparison between the current study and another similar study for GFRP bars exposed to high alkaline is presented in Figure 5.15. A high tensile strength reduction was expected after testing the bars; however, the trend line for this study showed an increase in the tensile strength. No clear explanation is evident for this case and further investigation should be done. This phenomenon may be attributed to the slow reaction between the glass matrix of GFRP bars and the NaOH solution at the beginning of the exposure.

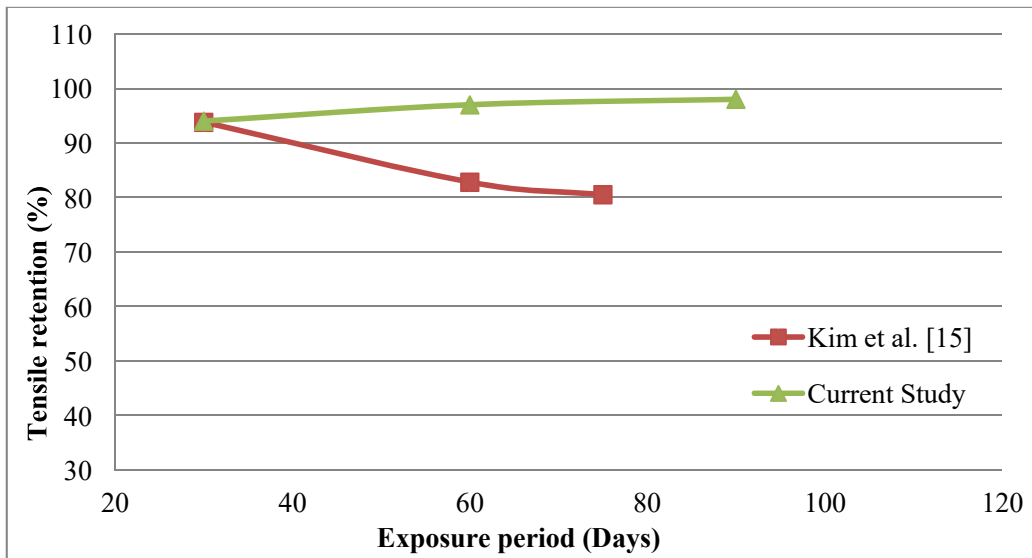


Figure 5.15: Retention of Tensile Strength of GFRP Bars Exposed to Alkaline Solution Compared to Previous Study

5.3. Arrhenius Modeling

Arrhenius modeling and time shift factors (TSF) are two approaches that can be utilized to predict the long-term behavior of GFRP bars [26].

Time shift factor is an equation that estimates the service life of GFRP bars by relating the accelerated and non-accelerated exposures. It can be used to extrapolate the accelerated data and obtain the long-term effects of the environment on the bars. The TSF value is measured between different temperatures and can be expressed by following equation [22]:

$$TSF = \exp \left[\frac{B}{T_1} \right] \exp \left[\frac{B}{T_2} \right] \quad (5.2)$$

where B is a constant that is determined using the time shift of two known curves and T1, T2 are temperatures between which the TSF is calculated (T1 is the lower temperature).

The TSF equation needs only two sets of data at different temperatures. TSF can be calculated by taking the ratio of the time required for the specific strength reduction from two

different temperatures and then substituting the values to give the B value. Thereafter, TSF can be found for any other temperature.

In the present research study, different exposures were tested for three different durations: 30, 60, and 90 days. Therefore, based on the short-term data from the accelerated tests, the Arrhenius model was implemented to predict the long-term behavior of the GFRP bars [5].

$$k = A \exp \left(\frac{-E_a}{RT} \right) \quad (5.3)$$

where k is the degradation rate (1/time), A is the constant of the material and degradation process, E_a is the activation energy, R is the universal gas constant, and T is the temperature in Kelvins.

Adopting the Arrhenius equation, a service life prediction can be obtained using accelerated aging data [26]. An accelerated aging test consists of two stages. First, FRP bars are exposed to different severe environments to accelerate the aging process. Second, longterm properties of the bars are predicted based on the accelerated test results. The strength retention versus time in logarithmic scale can be plotted using linear regression with the value of R^2 being at least 0.80, according to the ASTM D 3045 [27]. If the regression is not linear, the Arrhenius equation cannot be used [28]. This approach provided a good procedure for the prediction of the long-term performance of FRP materials. The main assumption of this model is that the degradation mechanism of the material will not change with time and temperature during the exposure, but the rate of degradation will be accelerated with the increase in temperature. The Arrhenius equation can be converted into Equation 5.4 which is the linear form of the Arrhenius model, where the logarithm of time needed for GFRP strength to reach a certain value is a linear function of $1/T$ with a slope of E_a/R [5].

$$\ln(t) = \frac{E_a}{R} \left(\frac{1}{T} \right) + \ln(A) \quad (5.4)$$

Figures 5.16-5.17 show the percentage retention vs. exposure duration for bond and tensile strength of the GFRP bars. Linear regression analysis was conducted for all exposures to fit a regression line through all sets of data with R^2 values higher than 0.8. All R^2 values were more than 0.88 except for the case of tensile strength for bars exposed to alkaline

solution. Hence, the relationship between service life and strength retention can be found through Arrhenius modeling.

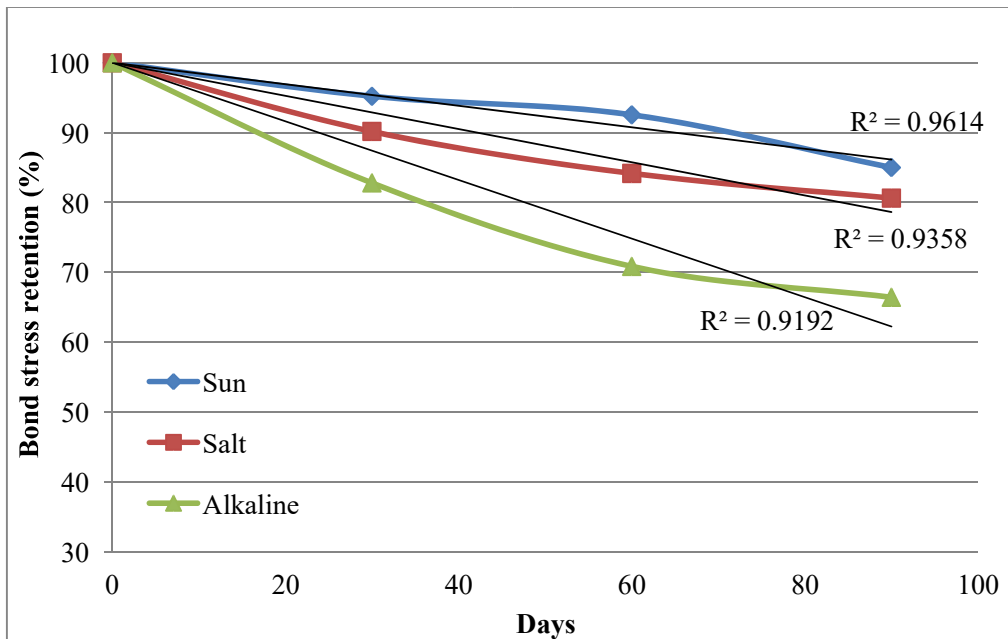


Figure 5.16: Regression Analysis for Bond Strength

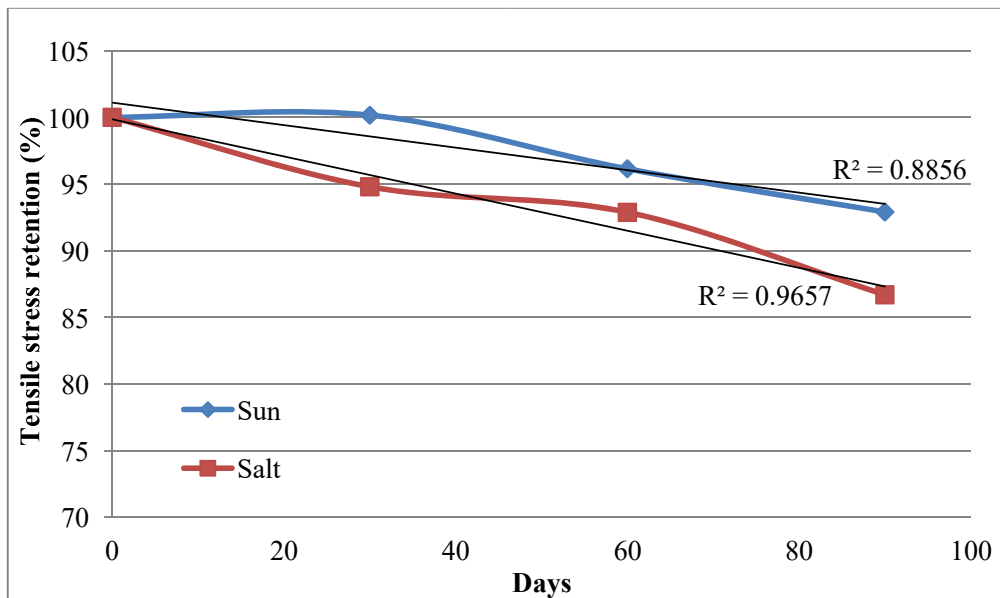


Figure 5.17: Regression Analysis for Tensile Strength

Long-term performance of GFRP bars can be predicted and plotted in two ways. The first method is by plotting the property percentage retention in linear scale versus time in logarithmic scale for different durations; the second is by plotting time as a function of inverse temperature for different property percentage retentions. Plotting the natural log of

retention time vs. the inverse of temperature in Kelvins gave the Arrhenius relationships shown in Figures 5.18-5.19. Straight lines were fitted to the data, as expressed in Equation 3, to obtain the E_a/R , which is the slope of the lines in the graphs.

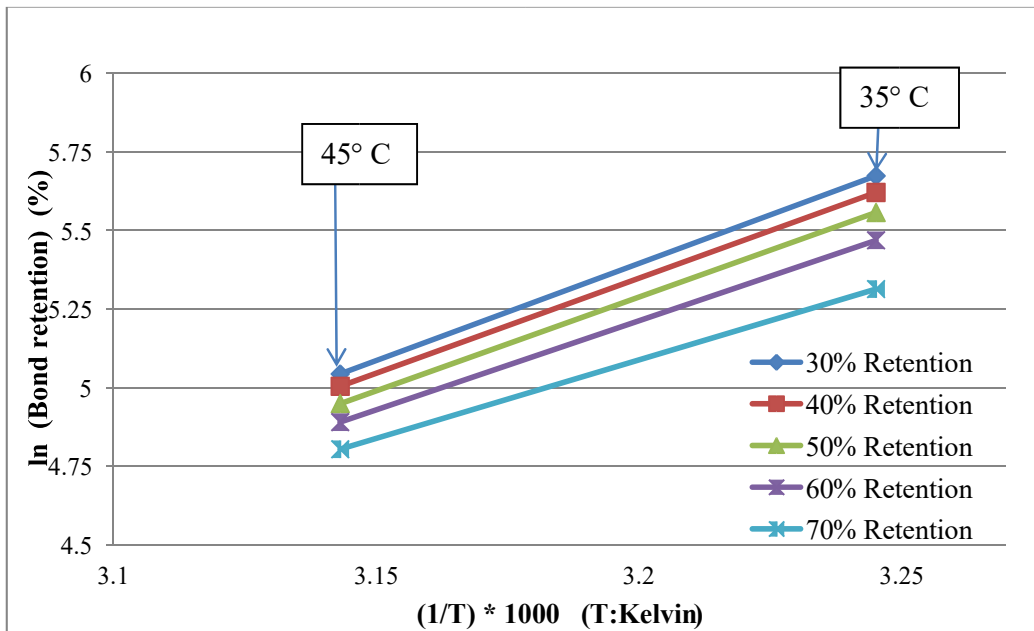


Figure 5.18: Arrhenius Plots of Bond Strength Degradation

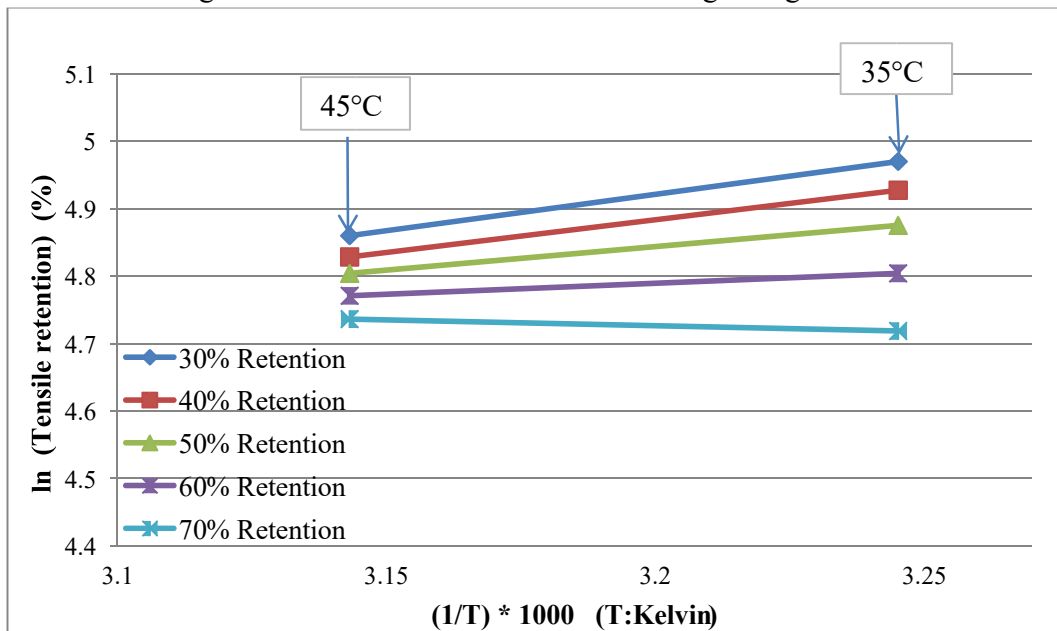


Figure 5.19: Arrhenius Plots of Tensile Strength Degradation

For predicting the long-term performance of GFRP bars, Figures 5.20-5.21 were plotted with exposure time on the horizontal axis in logarithmic scale, and the property retention value on the vertical axis using a linear scale.

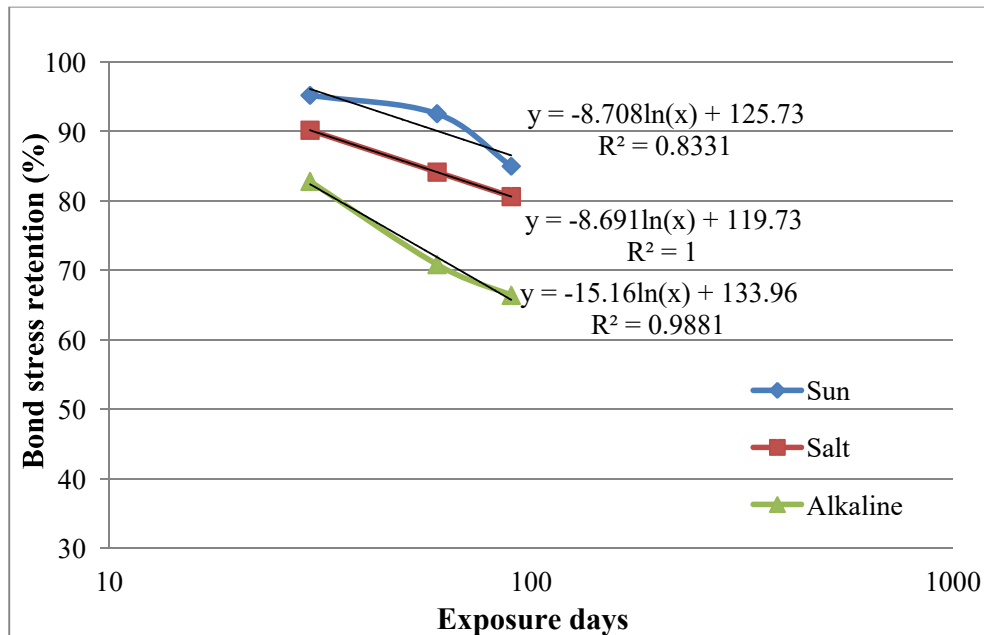


Figure 5.20: Long-term Performance of the Bond Strength of GFRP Bars

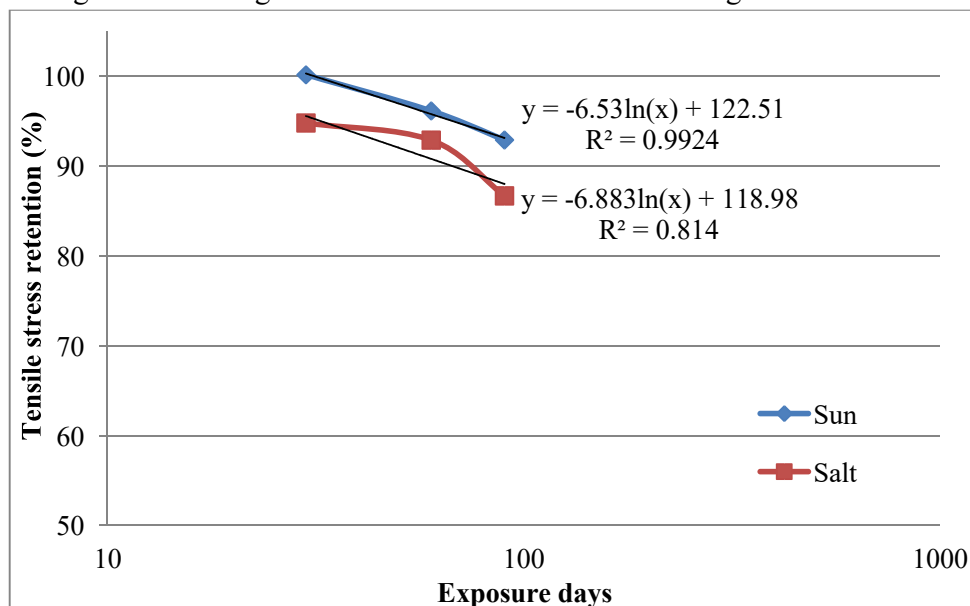


Figure 5.21: Long-term Performance of the Tensile Strength of GFRP Bars

Substitution of the values for strength retention in the logarithmic equation of each line gives the long-term properties for each type of exposure and for specific percentage retention. Table 5.3 is a summary of the results obtained from Arrhenius modeling.

Table 5.3: Service Life Prediction of GFRP Bars for Different Type of Exposures

Number of years it takes for GFRP bars to reach a certain strength		
	Type of exposure (bond)	Type of exposure (tensile)

% Retention	Sun	Salt	Alkaline	Sun	Salt	Alkaline
40	51.7	26.4	1.3	841.9	263.7	-
50	16.4	8.4	0.7	182.0	61.7	-
60	5.2	2.6	0.4	39.4	14.4	-
70	1.6	0.8	0.2	8.5	3.4	-
80	191 (days)	97 (days)	36 (days)	672 (days)	289 (days)	-
90	61 (days)	31 (days)	19 (days)	146 (days)	70 (days)	-

Chapter 6: Conclusions and Recommendations

6.1. Conclusions

The following conclusions can be derived from this research:

- All specimens tested by pullout tests failed by bond slipping through the free-end. Few concrete specimens also suffered cracks and/or small crushing in the bottom.

- Alkaline solution was the most severe environment for the GFRP bars. The strength reductions were 17.21%, 29.16%, and 33.59% at exposure of 30, 60, and 90 days, respectively. The seawater solution was the second most aggressive exposure, followed by the high temperature environment. The bond strength for GFRP bars exposed to high temperature was reduced by 4.8%, 7.5%, and 15.0% at 30, 60, and 90 days, respectively.
- GFRP bars showed no reduction in tensile strength during up to 30 days of hot and humid exposure. However there were reduction of 3.86% and 7.1% at 60 and 90 days respectively due to the same exposure. Alkaline solution exposure showed lower strength compared to the hot and humid exposure. However, the tensile strength was not reduced after increasing the exposure period. The seawater splash zone environment affected the GFRP bar strength more severely than the other exposures.
- There was an increase in the tensile strength for the specimens exposed to alkaline solution. It could be attributed to a complex short term chemical reaction that would develop between the glass matrix and NaOH solution. However this strength would be reduced in the long run for possible deterioration of the bond. More investigations are required to understand this behavior.
- Long-term performance behavior of the GFRP bars embedded in concrete was estimated according to Arrhenius modeling. The bond strength retains 90% of its full capacity after 61, 31, and 19 days when exposed to sun, seawater solution, and high alkali solution, respectively. Therefore it is recommended to store GFRP bars carefully in the site with minimum exposures in order to maintain their initial bond strength.
- It will take 146 and 70 days to fall below 90% of the initial tensile strength for bars exposed to sun and salt conditions, respectively. Alkaline exposure data could not fit the modeling to predict the long-term performance of the bars because R^2 value was less than 0.80.

- In structures such as parking garages, bridge decks, retaining walls, and marine structures, GFRP bars should be seriously considered as an alternative to steel in view of the extent of the deterioration due to corrosion of steel. However, protection of GFRP bars before using them should be considered because physical and mechanical properties of these bars would change due to long exposure to harsh environment.

6.2. Recommendations

The following is recommended for further studies:

- This research program tested only the bond and tensile strength of the GFRP bars. Additional research can be done on flexural behavior of concrete beams reinforced with GFRP bars after exposure to adverse environments.
- Arrhenius modeling can be validated by testing extra bars exposed for a longer period (1 or 2 years).

References

- [1] M. Robert and B. Benmokrane, "Behavior of GFRP Reinforcing Bars Subjected to Extreme Temperatures," *Journal of Composites for Construction*, vol. 14, pp. 353-360, 2010.

- [2] M. Schurch and P. Jost, "GFRP Soft-Eye for TBM Breakthrough: Possibilities with a Modern Construction Material," *International Symposium on Underground Excavation and Tunnelling*, 2006.
- [3] G. Nkurunziza, A. Debaiky, P. Cousin and B. Benmokrane, "Durability of GFRP bars: A critical review of the literature," *Progress in structural engineering and materials*, vol. 7, pp. 194-209, 2005.
- [4] J. Alves, A. El-Ragaby and E. El-Salakawi, "Durability of GFRP Bars' Bond to Concrete under Different Loading and Environmental Conditions," *ASCE*, pp. 249-262, 2011.
- [5] J. Zhou, X. Chen and S. Chen, "Durability and service life prediction of GFRP bars embedded in concrete under," *Nuclear Engineering and Design*, vol. 241, pp. 40954102, 2011.
- [6] A. S. Kamal and M. Boulfiza, "Durability of GFRP Rebars in Simulated Concrete Solutions under Accelerated Aging Conditions," *Journal of Composites for Construction*, no. 15, pp. 473-481, 2011.
- [7] ACI Committee 440.1R-01, "Guide for Design and Construction of Concrete Reinforced with FRP Bars.," *American Concrete Institute. Farmington Hills 440.1R-0*, 2001.
- [8] F. Micelli and A. Nanni, "Durability of FRP rods for concrete structures," *Construction and Building Materials*, vol. 18, pp. 491-503, 2004.
- [9] Y. Chen, J. F. Davalos, I. Ray and H. Kim, "Accelerated aging tests for evaluations of durability performance," *Composite Structures*, vol. 78, pp. 101-111, September 2007.
- [10] M. Robert and B. Benmokrane, "Effect of aging on bond of GFRP bars embedded in concrete," *Cement & Concrete Composites*, vol. 32, pp. 461-467, 2010.
- [11] A. Abbasi and P. J. Hogg, "Temperature and environmental effects on glass fibre rebar: modulus, strength and interfacial bond strength with concrete," *Composites: Part B*, vol. 36, pp. 394-404, 2005.
- [12] S. Tastani and S. Pantazopoulou, "Experimental evaluation of the direct tension-pullout bond test," *Bond in concrete—from research to standards*, pp. 1-8, 2002.
- [13] J. Zhou, X. Chen and S. Chen, "Durability and service life prediction of GFRP bars embedded in concrete under," *Nuclear Engineering and Design*, vol. 241, pp. 40954102, 2011.
- [14] R. Masmoudi, M. Ben Ouezdou, A. Daoud and A. Masmoudi, "Long-term bond performance of GFRP bars in concrete under temperature ranging from 20 oC to 80 oC," *Construction and Building Materials*, vol. 25, pp. 486-493, 2011.

- [15] H. Kim, Y. Park, Y. You and C. Moon, "Short-term durability test for GFRP rods under various environmental conditions," *Composite Structures*, vol. 83, pp. 37-47, 2007.
- [16] M. Porter and B. Barnes, "Accelerated durability of FRP reinforcement for concrete structures," *Durability of fiber reinforced polymer for construction*, pp. 191-201, 1998.
- [17] F. Gaona, "Characterization of design parameters for fiber reinforced composite reinforced concrete systems," 2003.
- [18] W. Chu, L. Wu and V. Karbhari, "Durability evaluation of moderate temperature cured E-glass/vinylester systems," *Composite Structures*, no. 66, p. 367–376, 2004.
- [19] M. Al-Zahrani, "Tensile strength degradation of glass fiber reinforced polymer bars in aggressive solutions both as stand-alone and cast-in-concrete," in *8th international symposium on fiber-polymer reinforcement for concrete structures*, 2007.
- [20] S. Alsayed, A. Alhozaimy, Y. Al-Salloum and T. Almusallam, "Durability of the new generation of GFRP rebars under severe environments," in *Durability of fiber reinforced polymer (FRP) composites for construction*, Montreal, 2002.
- [21] J. Won, Y. Yoon, B. Hong, T. Choi and S. Lee, "Durability characteristics of nanoGFRP composite reinforcing bars for concrete," *Composite Structures*, 2011.
- [22] Y. Chen, J. F. Davalos and I. Ray, "Durability Prediction for GFRP Reinforcing Bars Using Short-Term Data of Accelerated Aging Tests," *Journal of Composites for Construction, ASCE*, no. 10, pp. 279-286, 2006.
- [23] E. G. Nawy, *Reinforced Concrete, A Fundamental Approach*, 2009.
- [24] ACI Committee, "Guide Test Methods for Fiber-Reinforced Polymers (FRPs) for Reinforcing or Strengthening Concrete Structures," *ACI 440.3R-04*, 2004.
- [25] ASTM International, *Standard Test Method for Tensile Properties of Plastics*, Pennsylvania: ASTM Int'l, 2011.
- [26] J. Huang and R. Aboutaha, "Environmental Reduction Factors for GFRP Bars Used as Concrete Reinforcement: New Scientific Approach," *Journal of Composites for Construction*, pp. 479-486, 2010.
- [27] American Society for Testing and Material (ASTM), *Annual book of ASTM standards*, West Conshohocken, PA, USA, 2000.
- [28] L. C. Bank, T. R. Gentryb, B. P. Thompsona and J. S. Russella, "A model specification for FRP composites for civil engineering structures," *Construction and Building Materials 17*, p. 405–437, 2003.

Appendix

A. Temperature and Humidity

Table A.1: Variation of Temperature and Humidity during the Exposure of GFRP Bars

Date	Outside Temperature	Tank Temperature	Humidity (%)
20 May 2012	40.2	33.4	63
21 May 2012	40.5	34.2	57
22 May 2012	40.6	33.0	55
23 May 2012	40.4	33.9	55
24 May 2012	40.5	33.1	53
27 May 2012	39.4	32.8	48
28 May 2012	38.2	32.1	46

29 May 2012	39.1	34.0	48
30 May 2012	39.2	32.8	45
31 May 2012	40.4	34.5	45
3 June 2012	45.8	36.5	47
4 June 2012	44.8	36.3	49
5 June 2012	45.8	36.5	47
6 June 2012	44.8	36.3	49
7 June 2012	45	36.4	49
10 June 2012	45.4	36.5	50
11 June 2012	43.5	35.5	60
12 June 2012	44	35.3	45
13 June 2012	43.8	35.2	46
14 June 2012	43.6	34.8	42
17 June 2012	44	35.8	45
18 June 2012	44.5	36	40
19 June 2012	45.6	35.3	41
20 June 2012	45	33	48
21 June 2012	45.3	33	60
24 June 2012	44.3	33	55
25 June 2012	44.7	33.2	58

26 June 2012	44.3	33	55
27 June 2012	44.2	35	60
28 June 2012	40.6	34.3	60
1 July 2012	39.6	33	59
2 July 2012	42	35	59
3 July 2012	44.8	36	57
4 July 2012	45	35.8	59
5 July 2012	47	36.3	61
8 July 2012	47	38	63
9 July 2012	47.2	38	63
10 July 2012	46.9	37	54
11 July 2012	45	36.3	70

12 July 2012	46	36.7	71
15 July 2012	47	37.4	71
16 July 2012	47.5	37.2	71
17 July 2012	47.3	37.4	71
18 July 2012	47.8	38.5	72
19 July 2012	48.1	38.4	75
22 July 2012	48.4	38.5	73
23 July 2012	48.1	37.6	72
24 July 2012	48.4	37.6	77
25 July 2012	49.1	37.8	79
26 July 2012	48	37.2	70
29 July 2012	48.37	37	72
30 July 2012	48.7	37	70
31 July 2012	48.4	36.8	72
1 August	47.6	37	72
2 August	47.6	35.1	73
5 August	46.5	35.3	65
7 August	47	36.7	63
9 August	45	36.4	69
12 August	46.5	35.8	70
14 August	47	36	75
16 August	47.7	36.3	78
19 August	46.5	36.2	82
21 August	46.0	36.8	80
23 August	46.7	37	76
26 August	46.0	36	65
28 August	45.2	35.5	63
30 August	45.5	35.5	62
2 September	44.7	34.8	57
4 September	44.8	34.5	58
6 September	44.0	34.2	55
9 September	43.2	33.5	60

11 September	42.5	33.2	58
13 September	41.8	33	68
16 September	41.7	31.9	66
18 September	40.2	32.1	60
20 September	40	32	58
23 September	40.5	32.3	59
25 September	41	31.9	60
27 September	39.5	31.5	63
30 September	41	32.3	60
2 October	38	29.2	57
4 October	37.3	29.3	52
7 October	37.5	29	50
9 October	35.2	28.7	45
11 October	34.6	28.9	49
14 October	35.2	28.3	54
16 October	36.8	27.9	53
18 October	35.5	27.2	52
21 October	34	27	52

B. Pullout Test Graphs

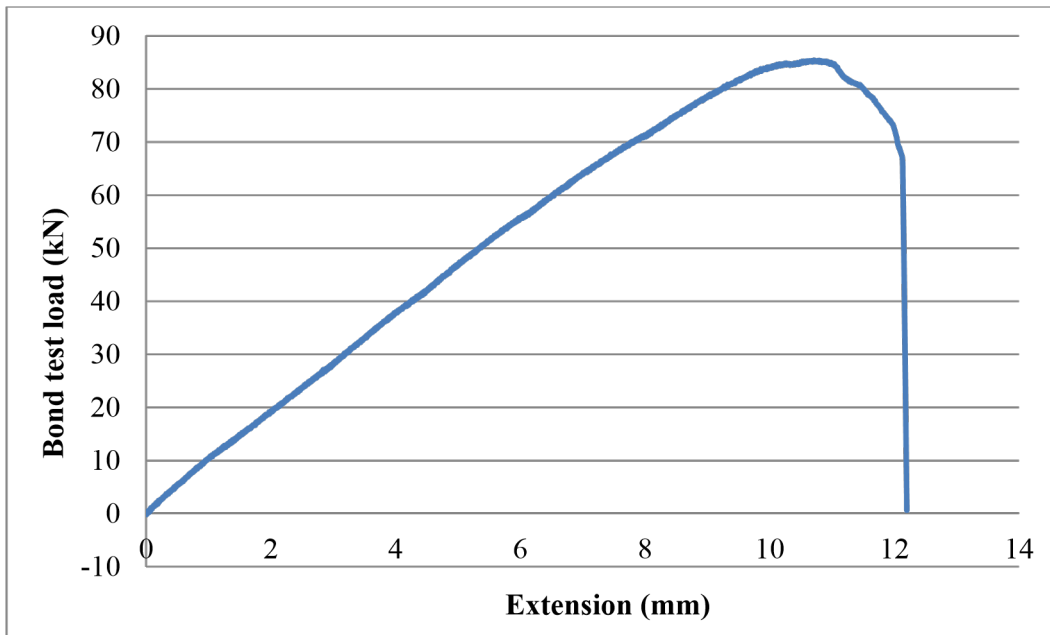


Figure B.1: Load-Extension Relationship of Unexposed GFRP Bar (Sample 1)

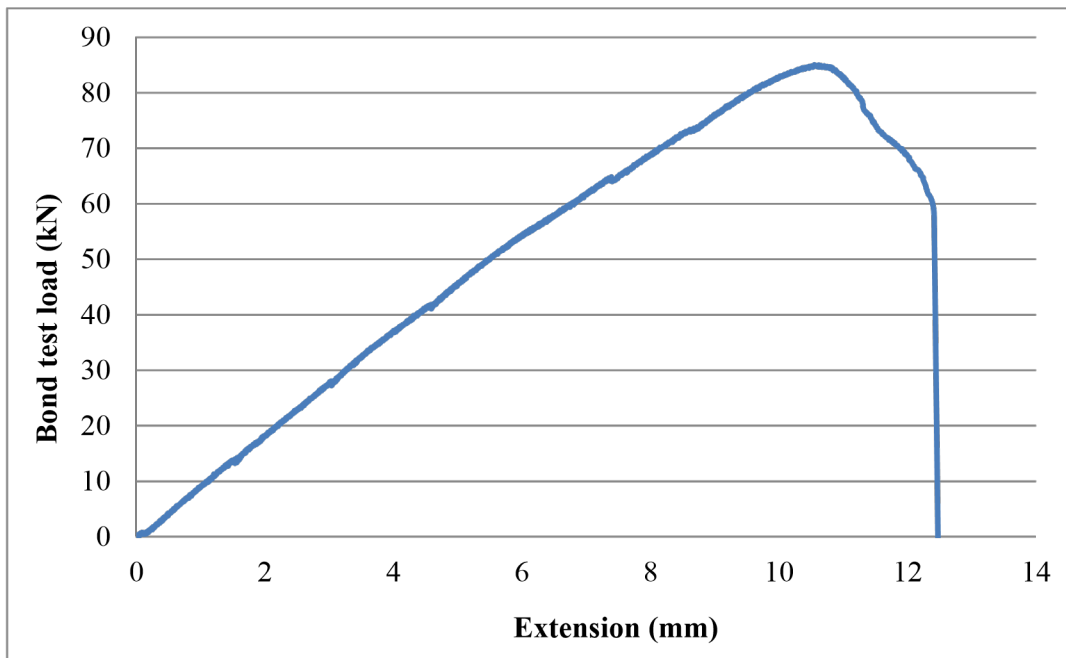


Figure B.2: Load-Extension Relationship of Unexposed GFRP Bar (Sample2)

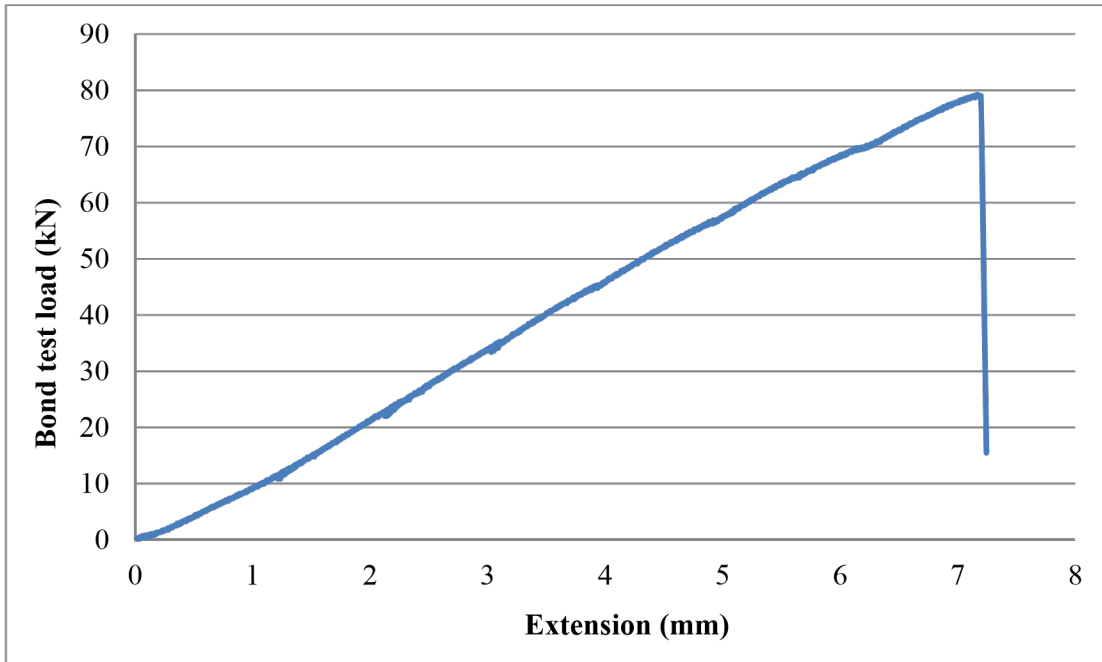


Figure B.3: Load-Extension Relationship of GFRP Bar Exposed to the Sun after 30 Days (Sample 1)

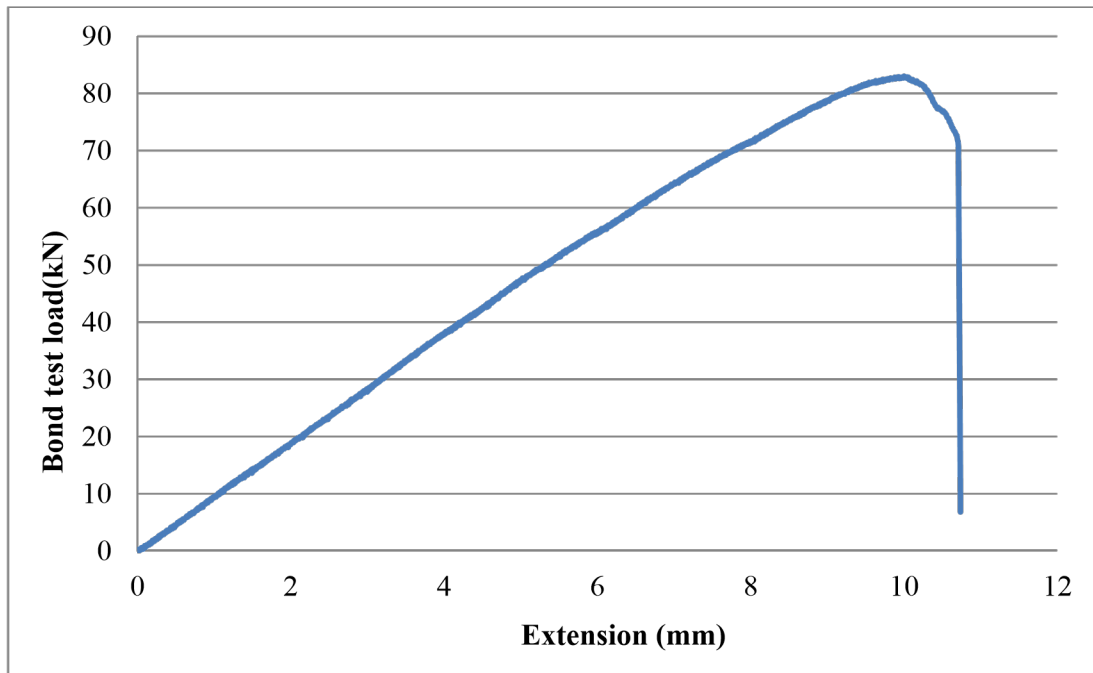


Figure B.4: Load-Extension Relationship of GFRP Bar Exposed to the Sun after 30 Days (Sample 2)

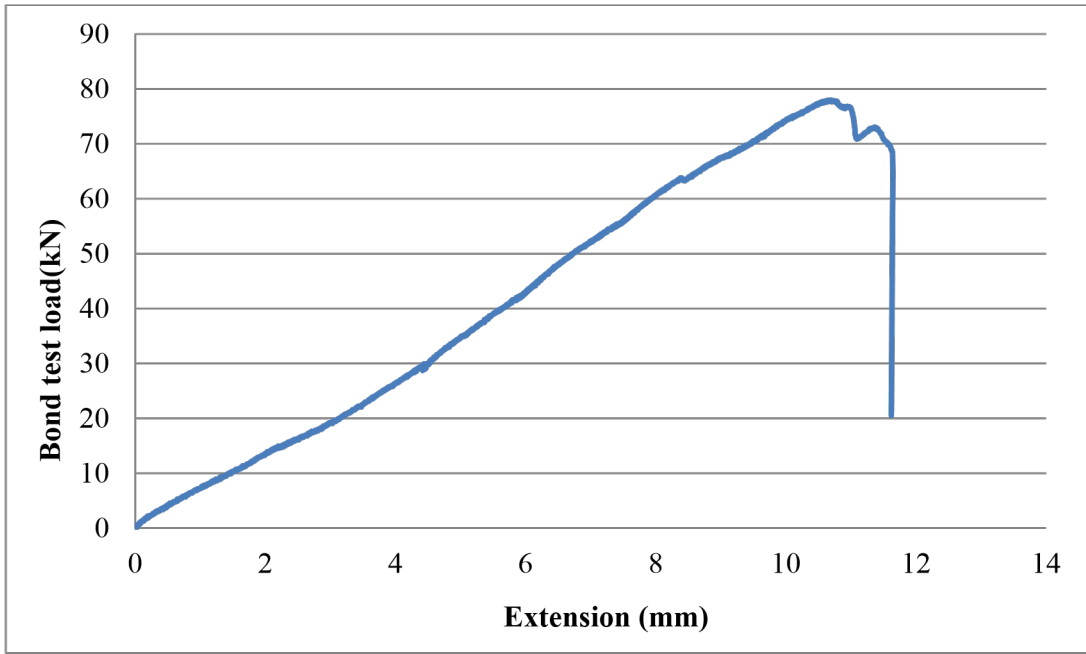


Figure B.5: Load-Extension Relationship of GFRP Bar Exposed to the Sun after 60 Days (Sample 1)

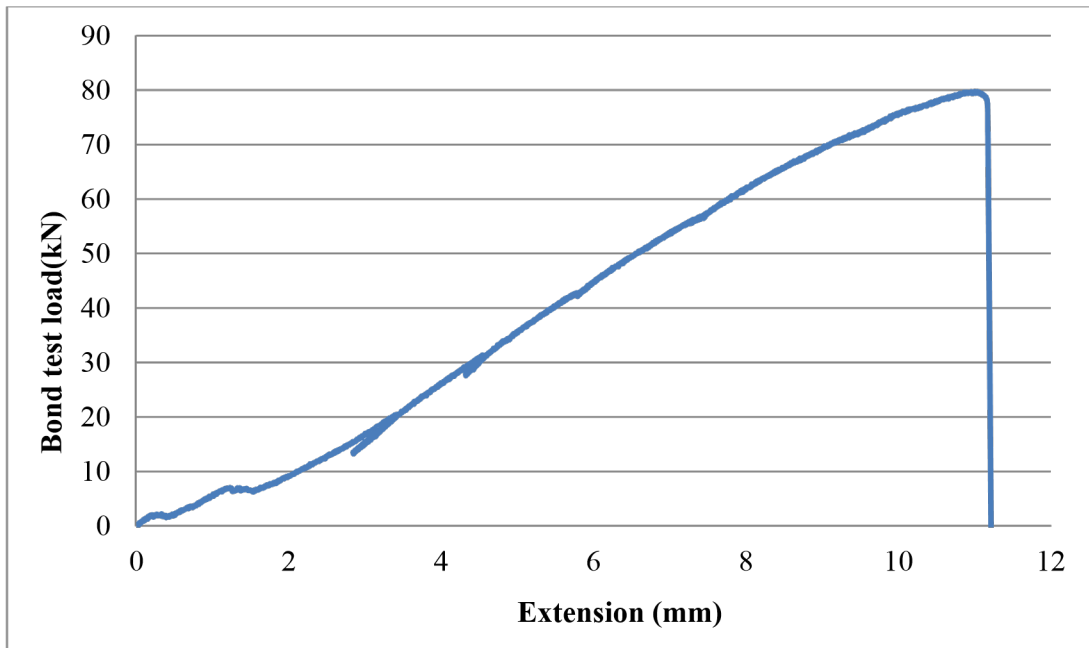


Figure B.6: Load-Extension Relationship of GFRP Bar Exposed to the Sun after 60 Days (Sample 2)

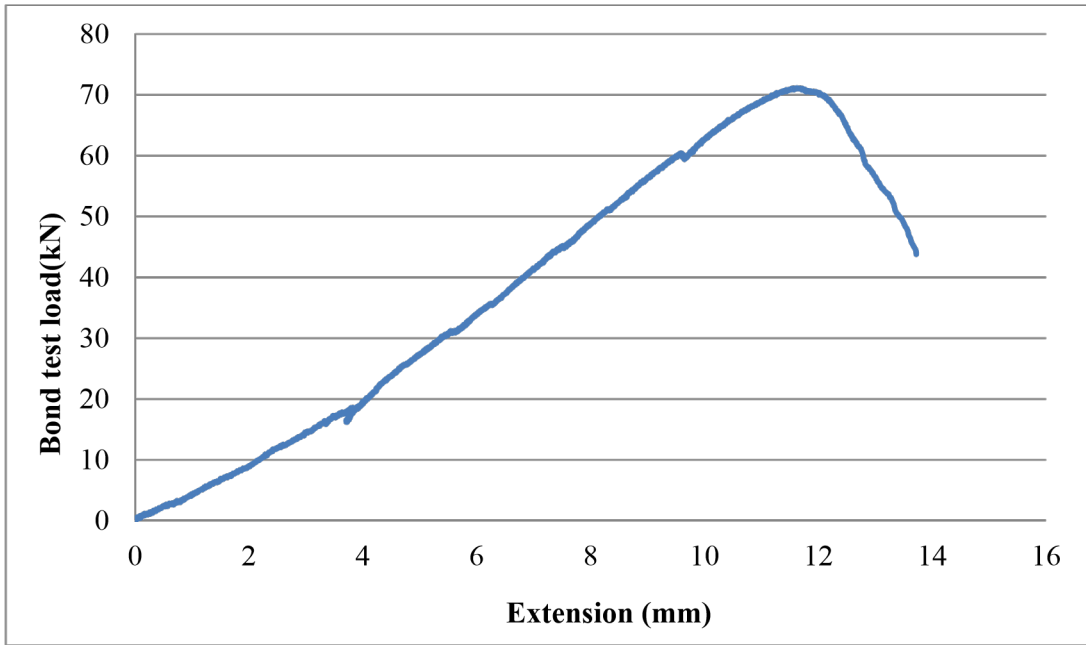


Figure B.7: Load-Extension Relationship of GFRP Bar Exposed to the Sun after 90 Days (Sample 1)

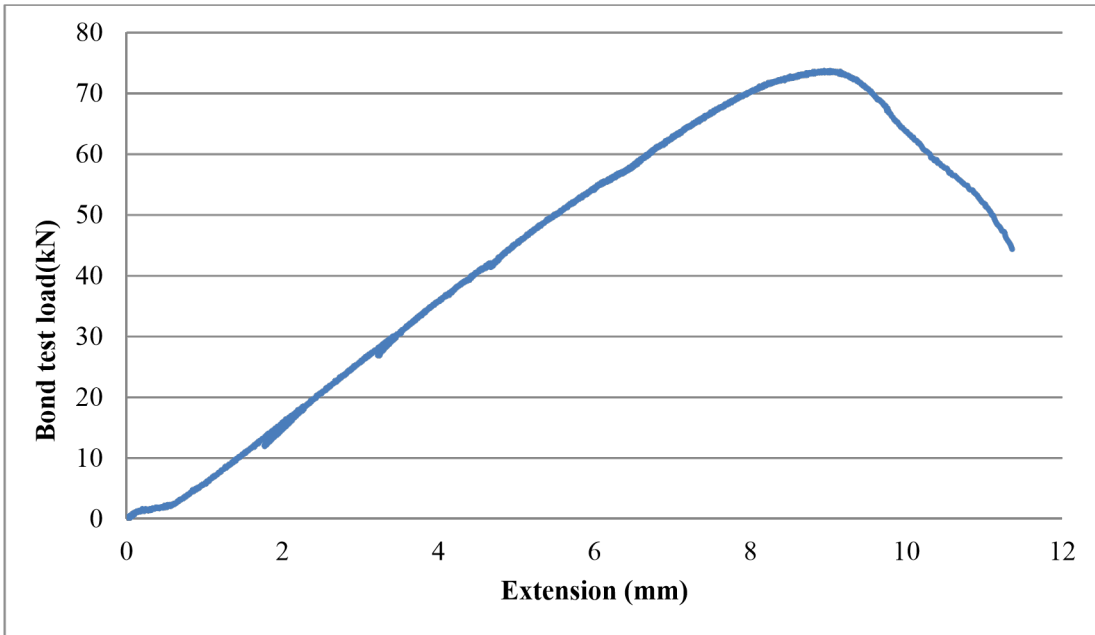


Figure B.8: Load-Extension Relationship of GFRP Bar Exposed to the Sun after 90 Days (Sample 2)

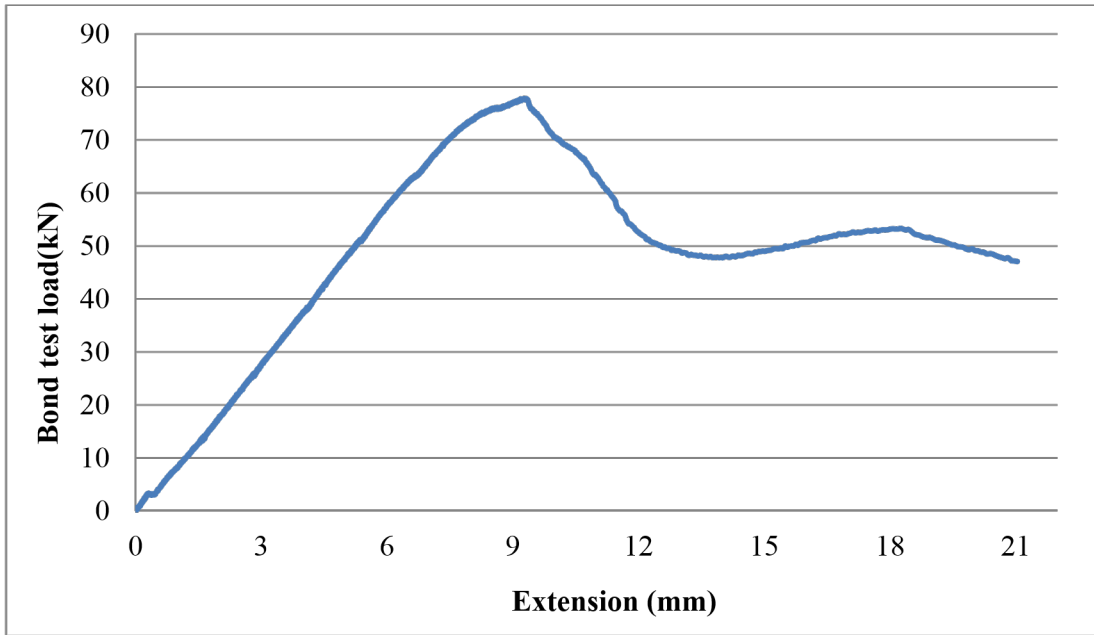


Figure B.9: Load-Extension Relationship of GFRP Bar Exposed to the Salt Solution after 30 Days (Sample 1)

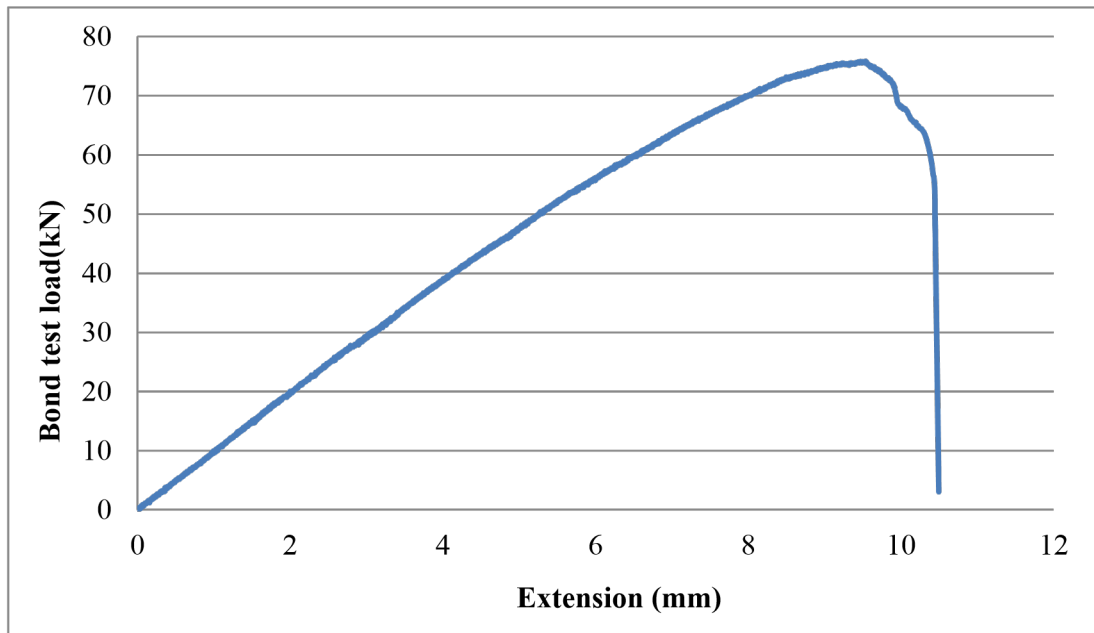


Figure B.10: Load-Extension Relationship of GFRP Bar Exposed to the Salt Solution after 30 Days (Sample 2)

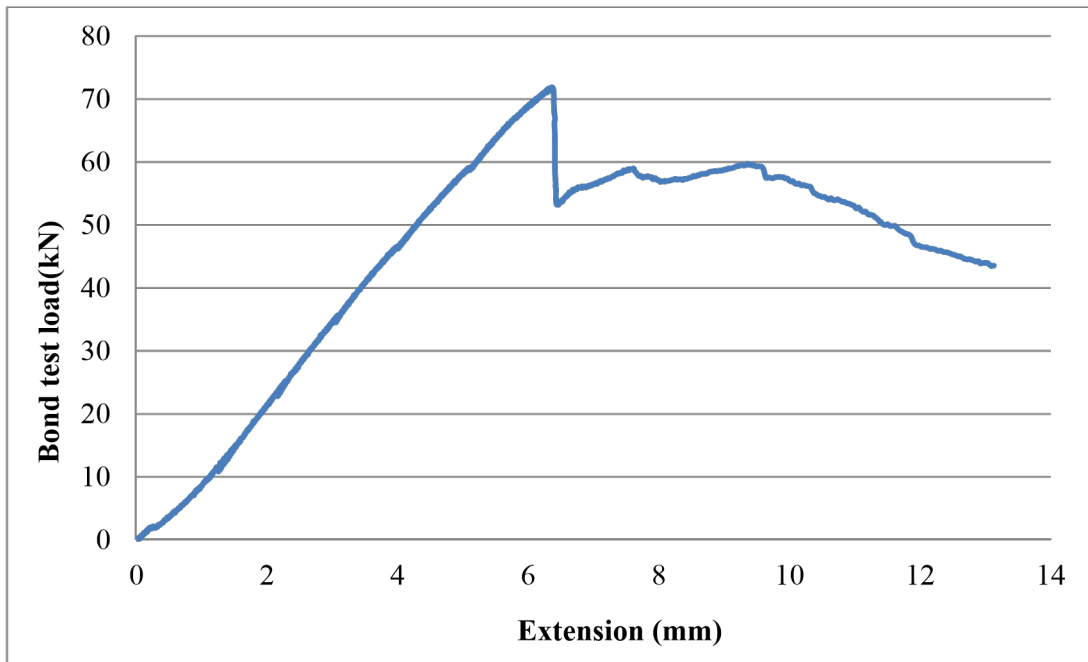


Figure B.11: Load-Extension Relationship of GFRP Bar Exposed to the Salt Solution after 60 Days (Sample 1)

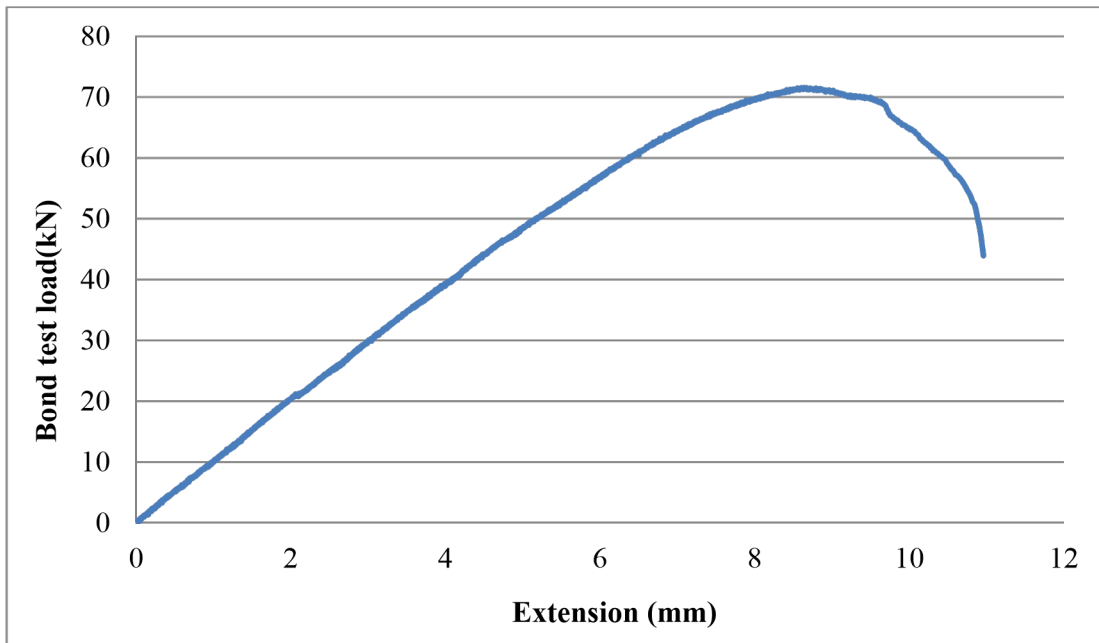


Figure B.12: Load-Extension Relationship of GFRP Bar Exposed to the Salt Solution after 60 Days (Sample 2)

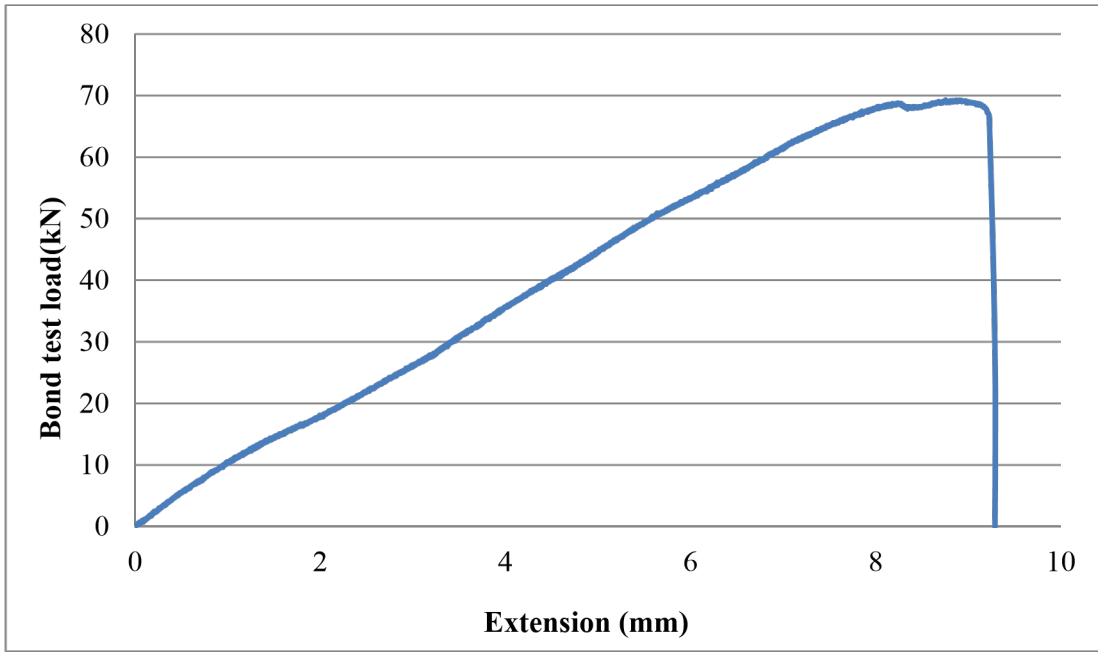


Figure B.13: Load-Extension Relationship of GFRP Bar Exposed to the Salt Solution after 90 Days (Sample 1)

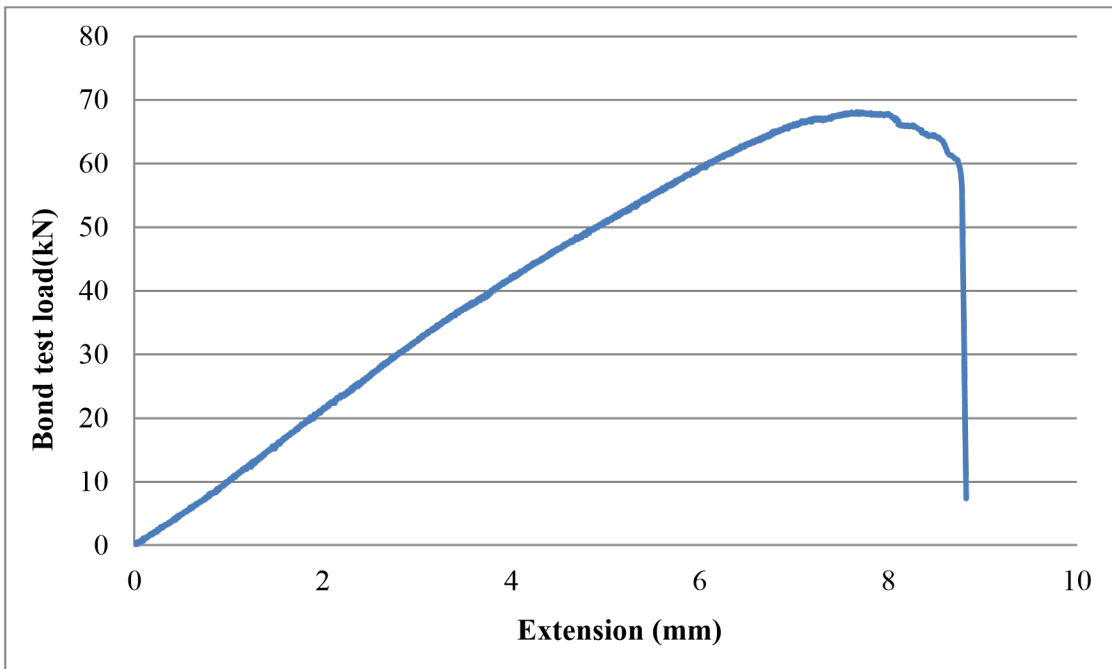


Figure B.14: Load-Extension Relationship of GFRP Bar Exposed to the Salt Solution after 90 Days (Sample 2)

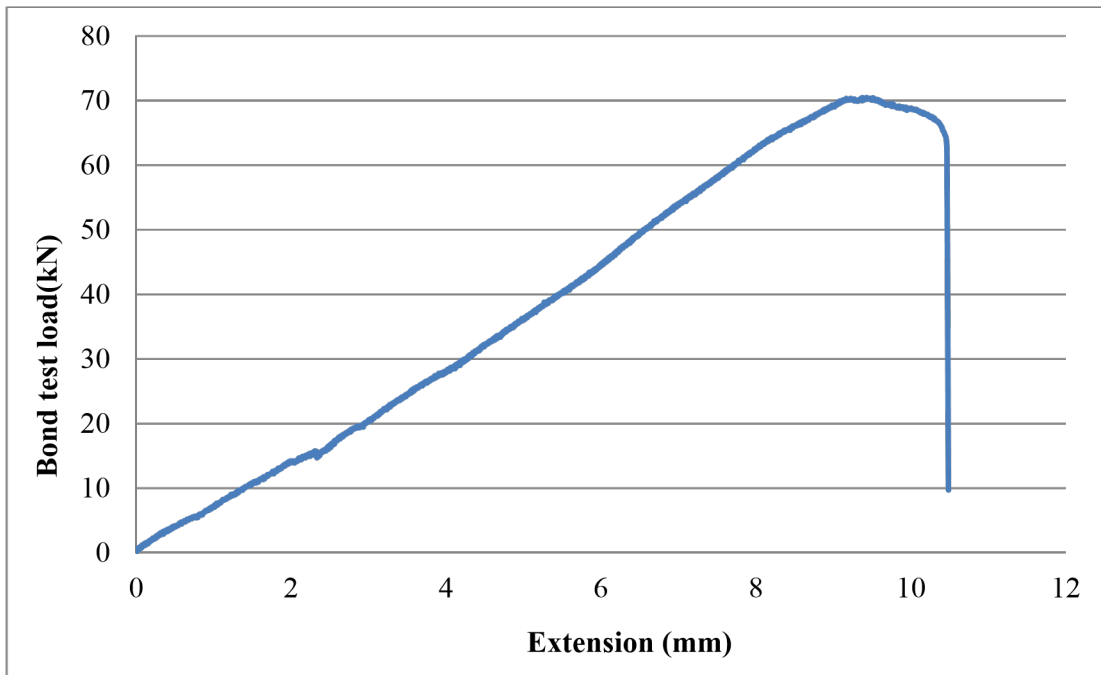


Figure B.15: Load-Extension Relationship of GFRP Bar Exposed to the Alkaline Solution after 30 Days (Sample 1)

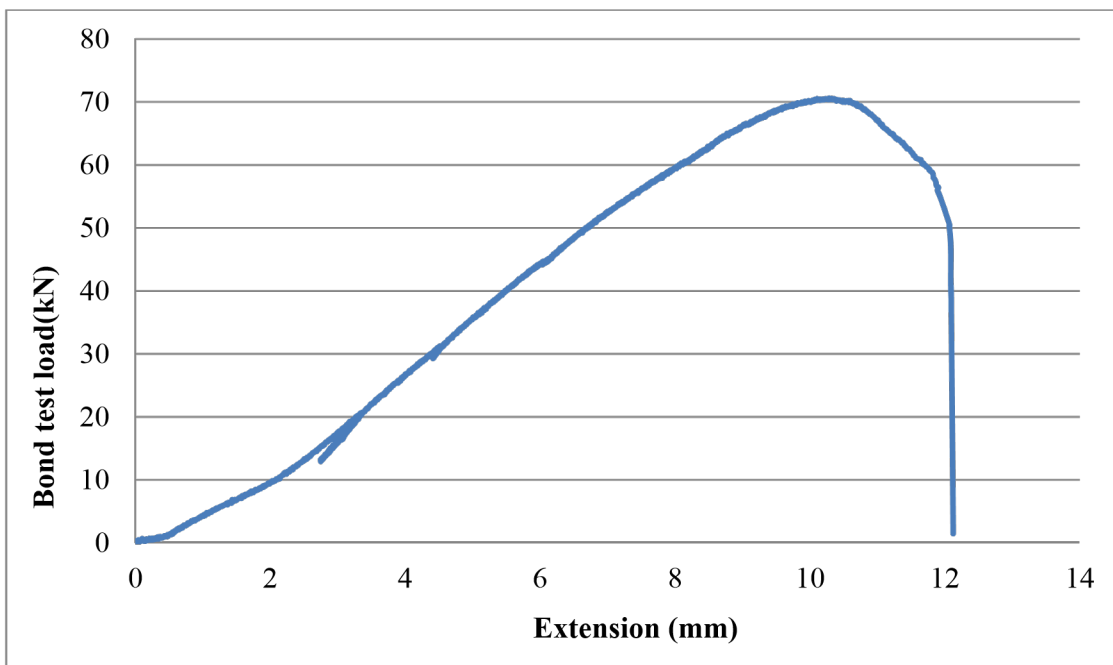


Figure B.16: Load-Extension Relationship of GFRP Bar Exposed to the Alkaline Solution after 30 Days (Sample 2)

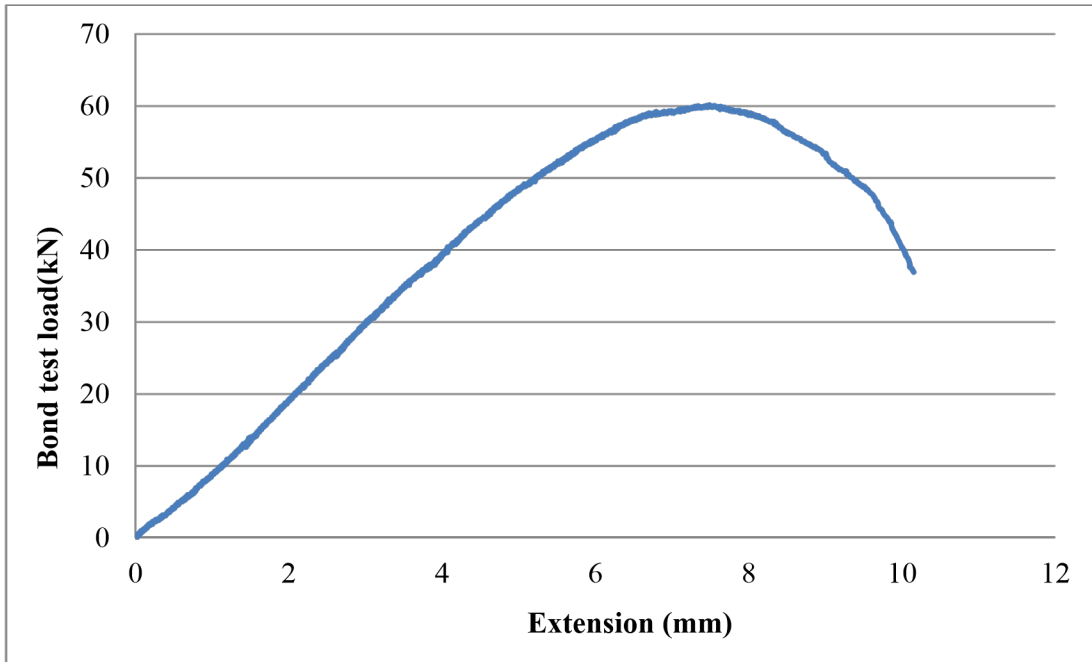


Figure B.17: Load-Extension Relationship of GFRP Bar Exposed to the Alkaline Solution after 60 Days (Sample 1)

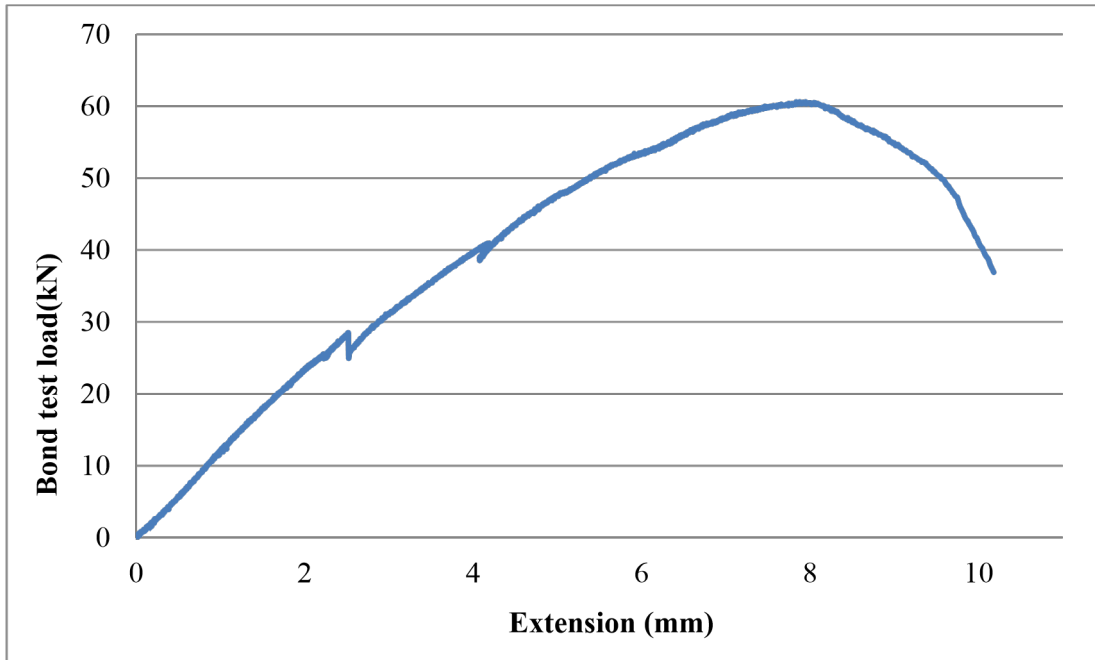


Figure B.18: Load-Extension Relationship of GFRP bar Exposed to the Alkaline Solution after 60 Days (Sample 2)

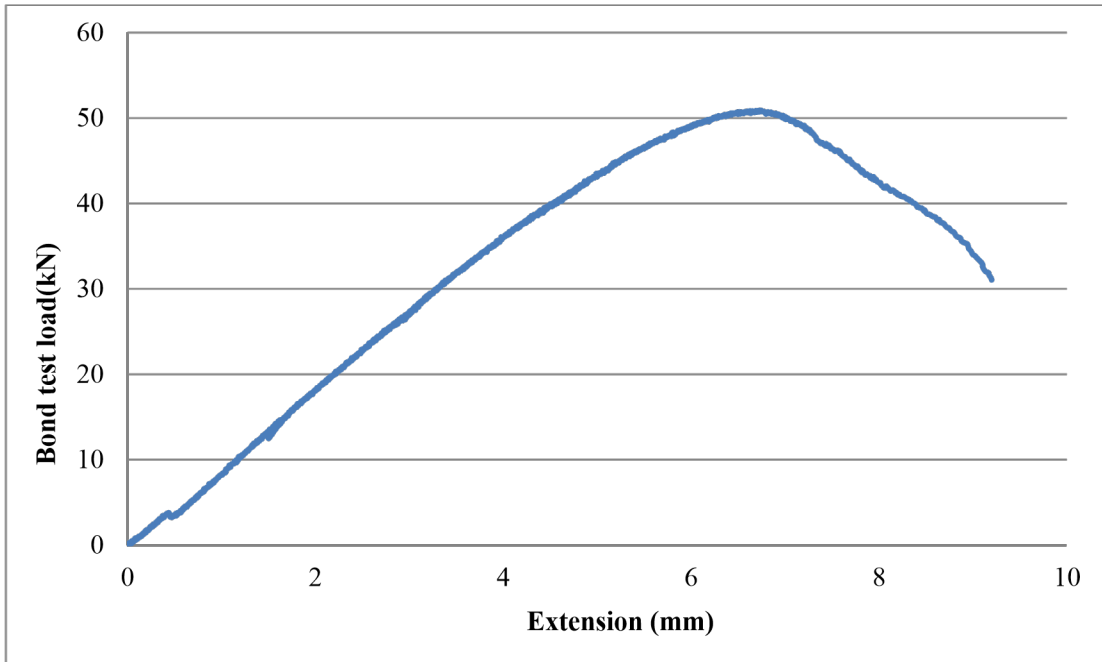


Figure B.19: Load-Extension Relationship of GFRP bar Exposed to the Alkaline Solution after 90 Days (Sample 1)

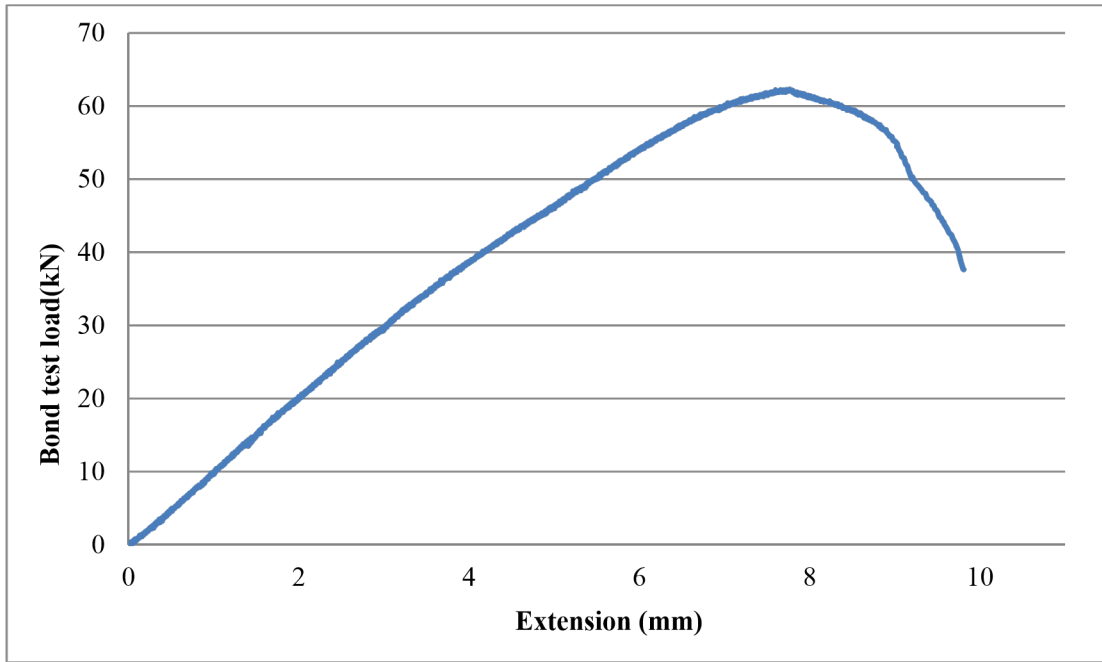


Figure B.20: Load-Extension Relationship of GFRP bar Exposed to the Alkaline Solution after 90 Days (Sample 2)

Vita

Saber Abedi was born on December 7, 1987, in Dubai, UAE. He started his education at the Towheed Iranian Primary School in Dubai, and he graduated from Towheed Iranian High School in 2005.

He continued his education at the American University of Sharjah and graduated in August 2010 with a B.S. degree in Civil Engineering. In 2010, he started his graduate studies at the American University of Sharjah in the Master's program in Civil Engineering Science. During his studies, he worked as a research and teaching assistant. He was in charge of several courses and performed lab duties primarily in the surveying and construction material laboratory. He is expected to receive the M.S. degree in Civil Engineering in January 2014.